For purposes of this application, including but not limited to, the Summary of the Invention, the Brief Description of the Drawings, the Detailed Description, the Claims, and the Abstract, the term "photovoltaic layer" shall be defined to include a layer of material having the characteristic and ability to receive and absorb electromagnetic radiation and to generate a current, namely a photocurrent, through the absorption of the electromagnetic radiation; the term "photovoltaic element" shall be defined to include a photovoltaic layer and one or more other functional layers or components, such as window layers, anti-reflective coatings, conduction layers, or metallic contacts; and the term "multi-element photovoltaic cell" shall be defined to include a photovoltaic cell having two or more photovoltaic elements. The term "electromagnetic radiation" includes particularly the ultraviolet, visible light and infrared spectrums respectively.

An objective of the present invention is to provide a multi-element photovoltaic cell having a photovoltaic controller, which provides for the continuous production of current by each of the irradiated photovoltaic cells of a photovoltaic array regardless of the level of irradiation.

A further objective of the device and method of the present invention is to provide for the continuous production of current by a photovoltaic cell by avoiding increasing the voltage of the discharge circuit, at each of the photovoltaic cells, above Vmp.

A further objective of the present invention is to provide for the continuous and optimized production of energy by each of the photovoltaic elements of a photovoltaic cell assembly while simultaneously stepping up the voltage of an aggregate current discharged by the photovoltaic cell assembly to a level required for discharge to an inverter or to a DC battery storage system, or both.

A further objective of the present invention is to provide for the continuous and optimized production of energy by each of the photovoltaic cells of a photovoltaic array while simultaneously stepping up the voltage of an aggregate current discharged by the full photovoltaic array to a level required for discharge to an inverter or to a DC battery storage system, or both.

Summary OF THE INVENTION

The multi-element photovoltaic cell of the present invention may have two or more photovoltaic elements with an isolation layer interposed between all contiguous photovoltaic elements. Also, regardless of the number of photovoltaic elements, each photovoltaic element will have an element front conductor and an element rear conductor which are in electrical contact with the photovoltaic layer of the photovoltaic element. There may also be an anti-reflective coating at the element front of each photovoltaic element. A rear insulation layer may electronically isolate the multi-element photovoltaic cell from its environment.

The first element front conductor must be optically transparent, including the ultraviolet and infrared wavelengths within the overall bandgap, and must be electrically conductive. It should have a high transmissivity for the portion of the electromagnetic radiation spectrum to be used for power generation, namely the portion of the incident solar radiation having a wavelength falling within the overall bandgap radiation for the photovoltaic cell, which includes the bandgap radiation falling within the element bandgap for each photovoltaic element.

11

Regardless of the number of photovoltaic elements, each element front conductor and each element rear conductor should have a high transmissivity for the transient bandgap radiation that it must pass to the following photovoltaic elements, with the exception of the last rear conductor of the last photovoltaic element.

Whether the photovoltaic cell is a two element cell, a three element cell, or has more than three elements, for a preferred embodiment of the photovoltaic cell assembly of the present invention, the current from a respective photovoltaic element which is generated as incident solar radiation irradiates the photovoltaic cell, flows independently of the other photovoltaic elements to at least one cell capacitor.

Solar radiation, which may include visible light and portions of the ultraviolet spectrum and the infrared spectrum, is incident to the photovoltaic cell assembly which is comprised of a plurality of photovoltaic elements. The photons of the solar radiation strike the absorption medium in each of the photovoltaic elements, thereby resulting in the release of electrons by the absorption medium of the photovoltaic elements. The resultant current will continue so long as the receiving voltage of the receiving circuit is less than the shut-down voltage, and so long as the photovoltaic cell is being irradiated by incident solar radiation.

For certain preferred embodiments of the photovoltaic cell of the present invention a transparent conducting film, such as a transparent conducting oxide may be used for the element transparent conductors. Carbon nanotube networks graphene, or polymer networks are examples of materials that may also be used for one or more of the transparent conductors. Other materials of that type may be known to persons of skill in the art and other similar materials may likely be the result of future technological development.

An alternative to providing a transparent conducting film for the element conductors is to provide an element front conduction zone and an element rear conduction zone which are integral with the element. These respective conduction zones can be provided through a high or increased level of doping of the conduction zones thereby transforming the semiconductor material into a conduction zone. Isolation layers interposed between contiguous photovoltaic elements must a high transmissivity rate for the radiation that must be passed to the following photovoltaic elements, and must be electrically non-conductive.

A preferred embodiment of the photovoltaic controller circuit includes a photovoltaic controller, a capacitor network comprised of a plurality of capacitor banks. Each photovoltaic element is electrically connected to a capacitor bank by a capacitor charge circuit. Each of the capacitor banks may comprise a plurality of cell capacitors. A capacitor voltage sensor may be connected to each cell capacitor and continuously or frequently monitor the voltage across the capacitor.

The process of the selective and sequential charging and discharging of the respective cell capacitors of each photovoltaic cell may thus be controlled by the photovoltaic controller, based upon the voltage monitored by the voltage sensors. The photovoltaic controller may cycle between the cell capacitors based upon the level of irradiation of the photovoltaic cell, the resultant current production of the photovoltaic cell, and the voltages across the cell capacitors as measured by the voltage sensors.

The capacitor switches as controlled by the photovoltaic controller can provide for the photovoltaic elements of the photovoltaic cell, to be connected in parallel and with selected element of other cells to

12

equalize the voltage before they are switched to discharge in series, providing for stepping up the voltage. If not equalized, the lowest voltage differential would determine the current.

The output circuit provides for each photovoltaic element to be connected in series or parallel . For a preferred embodiment, the capacitor switches may be operated by the photovoltaic controller to provide for each group of photovoltaic cell capacitors that are to be discharged in series, to be first connected in parallel to provide for equalization of the voltage on each capacitor. This prevents the lowest voltage capacitor in the series from limiting the current when the capacitors are switched to discharging in series.

For capacitors connected in series, the current is the same at all points in the interconnecting circuit, and thus the current is the same to and from each capacitor. If independently charged capacitors are switched to series connection, the capacitor with the least voltage differential between the cathode and the anode at the time of the initial switching to a series configuration will determine the current flow from the series of capacitors. Further, the total charge discharged from the capacitor series, will be limited to the total charge stored in the capacitor of the series with the least total charge. Therefore, in order to maximize the discharge current and total charge discharged from independently charged capacitors of the same characteristics and capacitance, and hence the total energy discharged, the capacitors should be connected in parallel, immediately before connecting them in series, for equalization of the voltage and charge stored on each of the capacitors.

It is anticipated, based upon current technology, that the capacitors, switches, voltage sensors, and circuit connections between these components, will be components of an integrated circuit in which the photovoltaic cells are imbedded. The utilization of additional capacitors, switches and voltage sensors for embodiments with a larger number of capacitors for each photovoltaic cell, would certainly increase the cost of the photovoltaic controller of the present invention.

For preferred embodiments, the photovoltaic controller may receive continuous voltage measurements, or voltage measurements made at intervals, from the voltage sensors of each photovoltaic cell of a photovoltaic array, and use the voltage data to control the switches so as to attempt to optimize the output power production for the photovoltaic array, while providing for connecting the discharge output of each photovoltaic cell to the output circuit. The current flowing from each photovoltaic element, and each photovoltaic cell may also be measured continuously, or at intervals, by a cell current sensor, and the current data transmitted to the photovoltaic controller. This current data may be used, along with the voltage data, by the photovoltaic controller to attempt to optimize the output power production for each photovoltaic cell and for a photovoltaic array as a whole.

For a preferred embodiment, the photovoltaic controller may incorporate a digital computer and may communicate by wire or wireless with the capacitor voltage sensors to receive voltage measurements and may communicate by wire or wireless with the charge switches and the discharge switches to cause the switches to open and close as needed to manage the charging and discharging of the photovoltaic cell capacitors so as to optimize the energy extraction of the photovoltaic array and to control the voltage and other characteristics of the output from the photovoltaic array so as to appropriately interface with storage, electric grid or other application for the extracted solar energy. For a preferred embodiment, the capacitor switches may be operated by the photovoltaic controller to provide for each group of photovoltaic cell capacitors that are to be discharged in series, to be first connected in parallel to provide for equalization of the voltage on each capacitor. This prevents the lowest voltage capacitor in the series from limiting the current when the capacitors are switched to discharging in series.

13

The photovoltaic controller of the photovoltaic assembly of the present invention may also provide for the concurrent operation of a plurality of photovoltaic assemblies, such as would be present in a photovoltaic array. The photovoltaic assembly may receive voltage sensor signals from a plurality of other photovoltaic assemblies, such as for a photovoltaic array of which the photovoltaic assembly of the present invention is a component, and may generate charging signals and discharging switch control signals, which are directed to a plurality of photovoltaic cell assemblies of the present invention, as in a photovoltaic array. In general, the photovoltaic controller will operate element capacitor charging switches and element capacitor discharging switches for each of the photovoltaic cell assemblies so as to optimize the charge, power and total energy output of the photovoltaic array of which the photovoltaic assembly of the present invention is a component.

14

EXHIBIT H

New Solar Breakthrough May Compete with Gas
www.iaus.com

International Automated Systems, Inc. [IAUS] has developed a unique solar power technology that it believes will be the first to compete with gas, coal, and oil. Two primary issues have prevented solar power from replacing fossil fuels: The first obstacle is the high cost of equipment. Currently, solar power equipment is far too expensive to compete with fossil fuels. The second is production capacity. Even if the price of today's solar power technologies was in line to compete with fossil fuels, the production capabilities are so limited it would take decades to even scratch the surface of replacing fossil fuels.

IAUS's new solar power technology presents a breakthrough on both fronts. The company's unique solar power technology is priced to replace fossil fuels, and its annual production capabilities marginalize any other solar technology- making it perhaps, the energy sector's holy grail in a market currently grossing more than $3 trillion annually but fueled by less than 1% solar.
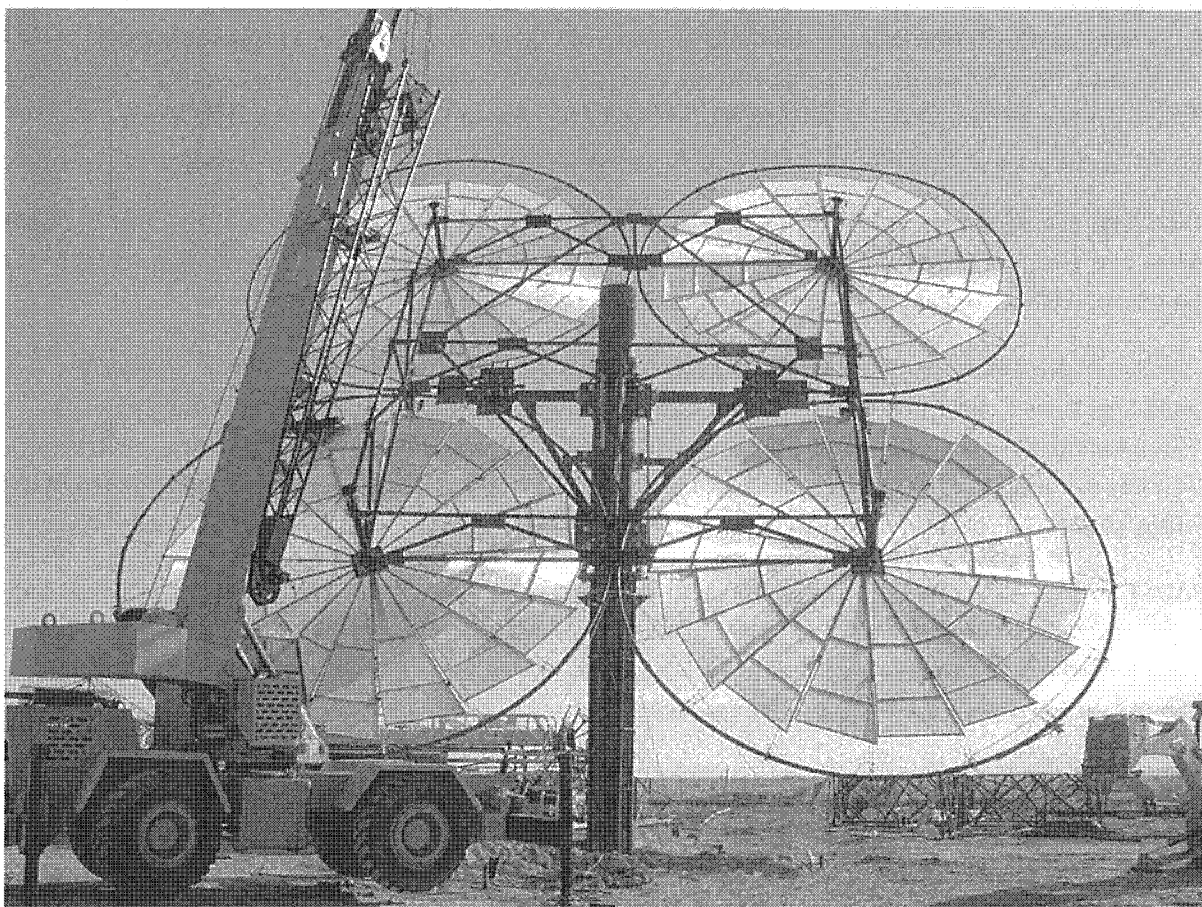
IAUS Solar Technology- What Makes it Different?

4

(Figure 1: IAUS Solar Tower with Four Circles of Panels)

IAUS Solar Panels- IAUS has developed a very unique thin panel with lens-like properties that focuses the sun's energy to a high-temperature focal point on a receiver.   The heat is converted to steam which is then used to generate electricity. IAUS'S unique panels are inexpensive, efficient, and low maintenance. Typical solar reflector panels (e.g. solar dishes, troughs, heliostats) are very expensive and require a great deal of periodic, manual fine-tuning to sustain a solar focal point on its target. Once installed, IAUS'S panels need no manual fine-tuning to maintain its focal point. This significantly reduces the cost of plant operation.

In addition to IAUS'S actual field tests, optical ray-tracing simulations have been conducted to verify the efficiencies of IAUS'S panel design. IAUS'S unique solar panels show efficiencies of over 90%. In the field, IAUS'S panels produce temperatures from 1,600-1,800 degrees Fahrenheit while tracking the sun.

By adding the new compound parabolic concentrator IAUS's temperature can exceed 2500°F.

Seventeen panels fit together in a circular pattern which spans approximately 39 feet in diameter. Four of these circles are mounted to a single tower equipped with dual-axis, automated tracking. The panels follow the sun east to west, north to south, producing higher number of hours than single axis concentrator solar power (CSP) systems and flat-plate mounted Photovoltaic (PV) systems.

IAUS'S unique panels are made up of a very durable, engineering grade monomer material that has been known to endure extreme weather conditions for more than 60 years with low degradation. IAUS'S panels are 100% recyclable.

The panels are also designed to rotate about themselves to reduce wind load on the system. As the wind approaches some predetermined velocity the panels will break loose and turn about there axis. This prevents the plastic panels from breaking while reducing wind load on the mechanical structure. This has the added advantage of reducing the metal in the mechanical structure thus reducing the cost of the structure. This also reduces maintenance cost in replacing broken lenses.

IAUS Receiver- Each circle of panels or lenses has only one receiver. There are four circles of lenses and four receivers per dual-axis tracking tower. The receiver is a heat-exchanger that directly transfers the heat from the high-temperature focal point into water. Water flows into each receiver until it reaches a temperature between 1,000-1,100 degrees Fahrenheit.

5
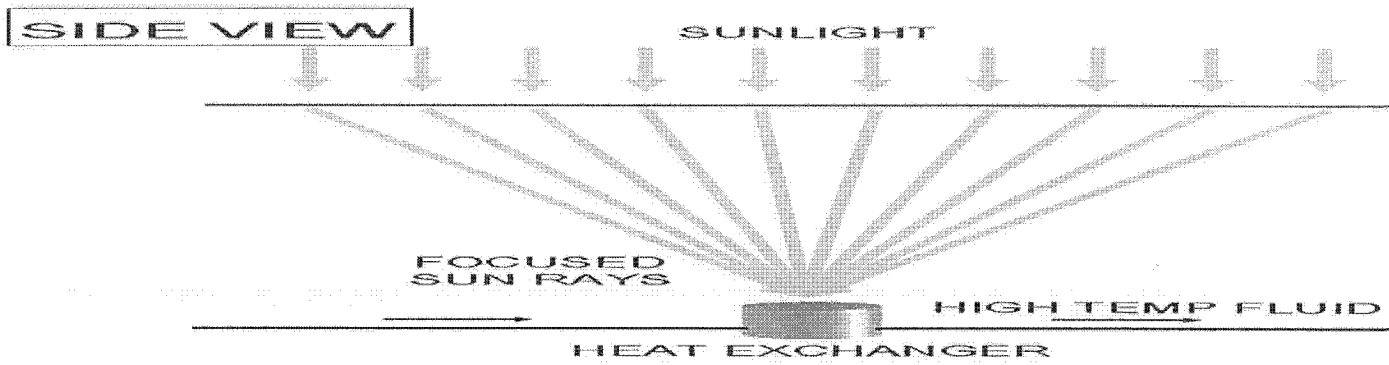
(Figure 2: Side view rendition of one of IAUS'S circle of solar panels or lenses focusing on a solar receiver heat exchanger)

In addition to performing field tests on its receivers, independent thermal dynamic and hydraulic flow simulations were conducted to verify flow rates and thermal efficiency.   These numbers supported that IAUS'S receiver has a heat-absorption rate efficiency of over 90%.
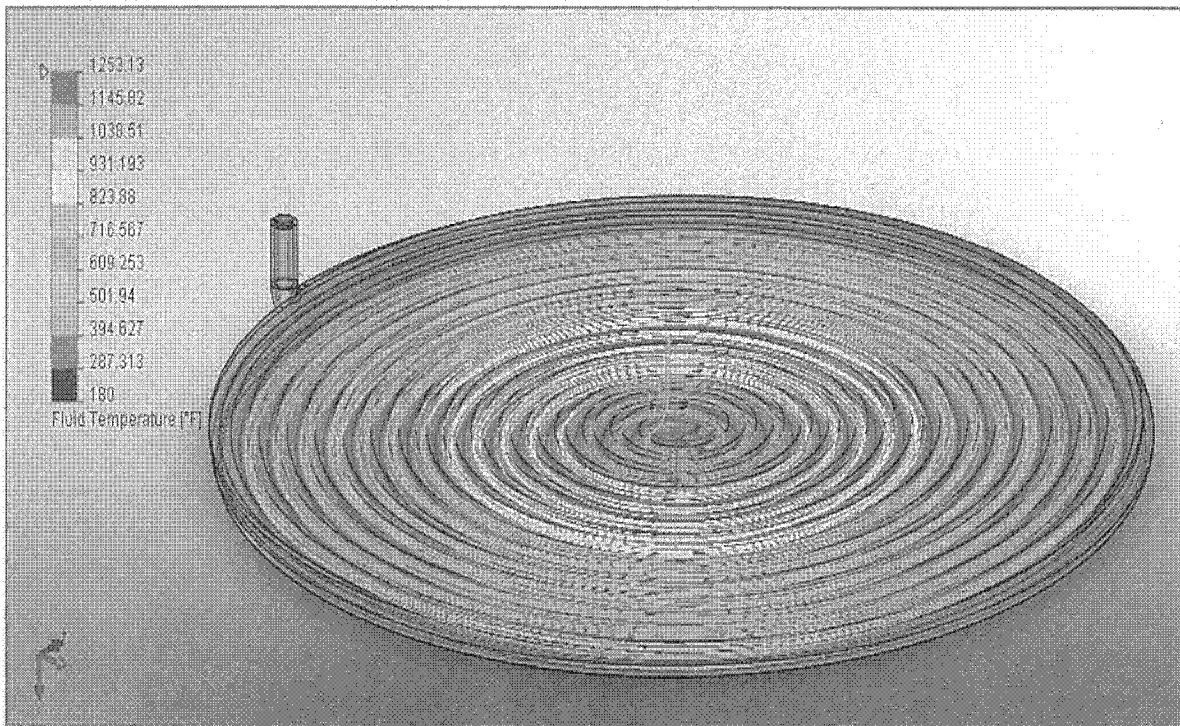
(Figure 3: Top cut section view of water absorbing the sun's heat through IAUS's solar receiver heat exchanger)

6
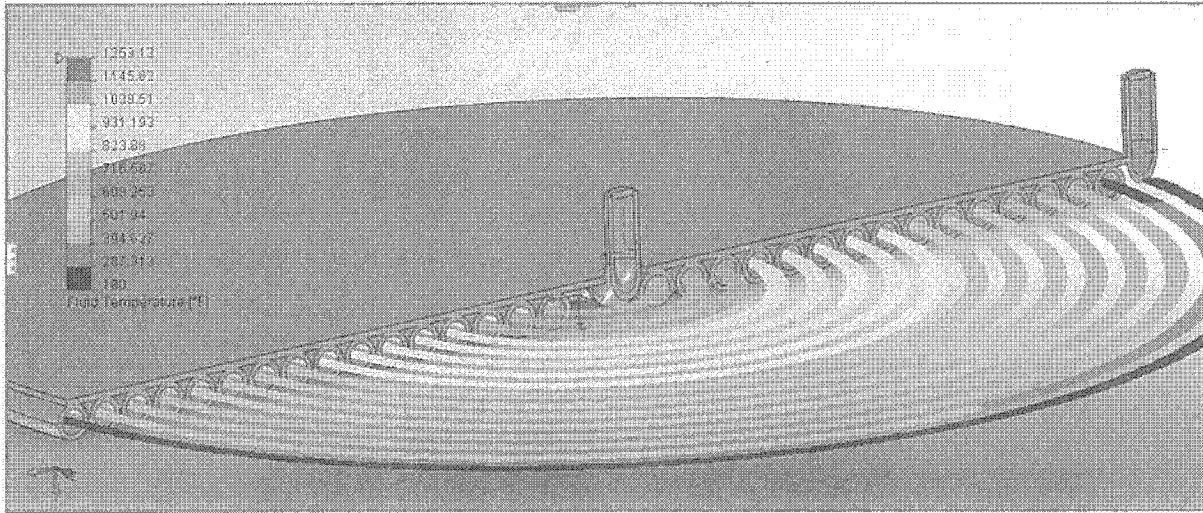
(Figure 4: Middle cut section view of water absorbing the sun's heat through IAUS's solar receiver heat exchanger)

7
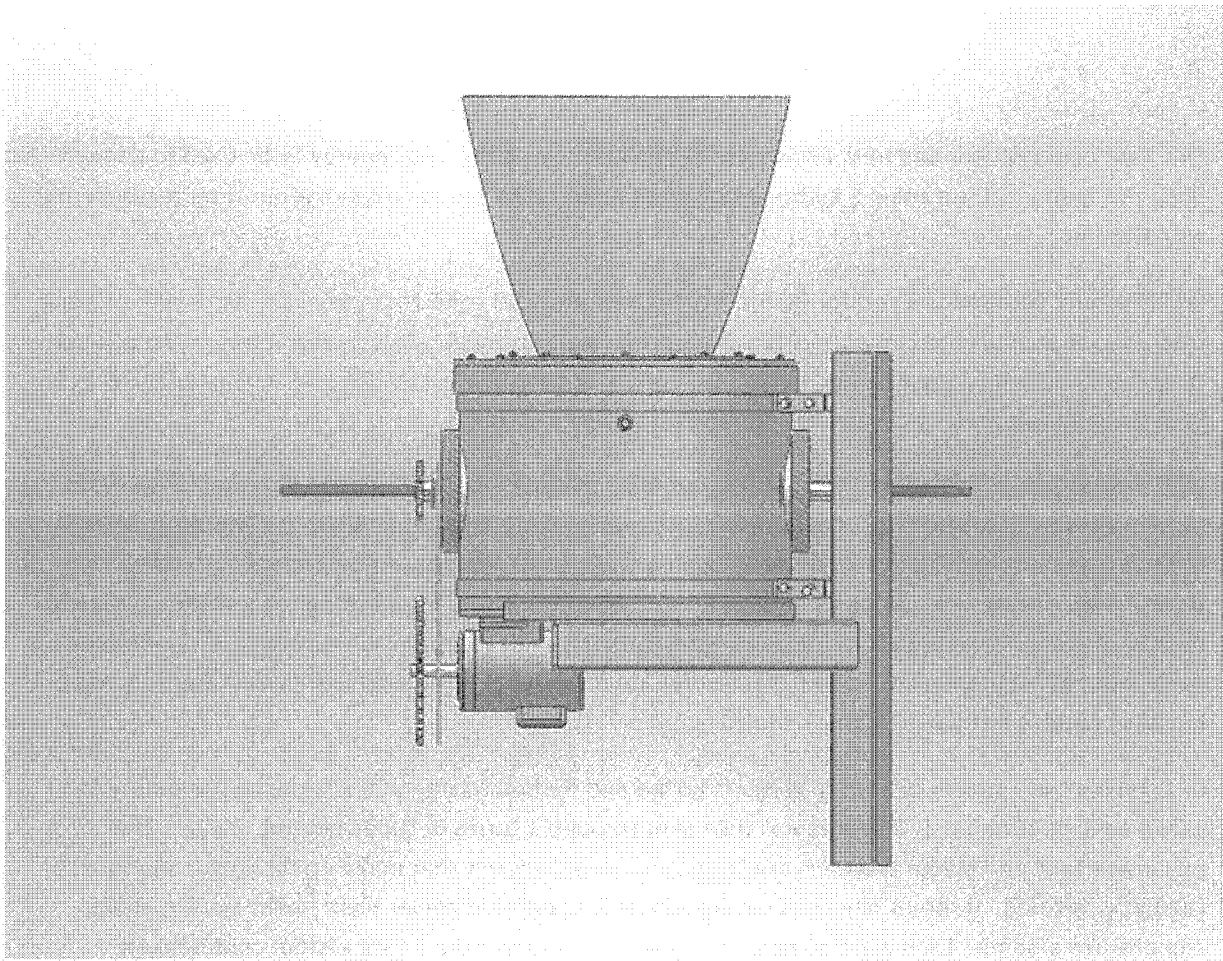
(Figure 4.1 New solar receiver showing the concentrator along with the movable heat exchanger)

New concentrator and heat exchanger- Referring to fig 4.1 this is the new heat exchanger design featuring the concentrator with the new heat exchanger and the rotation mechanism. The top portion is the concentrator which takes the incoming rays from the lens and further concentrates the suns rays which also increases the temperatures that hit the heat exchanger portion. The heat exchanger rotates to control the temperature at any given point on the heat exchanger. The rotation also eliminates hot spots on the heat exchanger reducing the chance of melting or burning the heat exchanger. This also provides a more even temperature exchange between the heat exchanger and the heat absorbing medium inside.

This heat concentrator and heat exchanger combination also reduces the infrared radiation coming off of the heat exchanger.

8

This heat concentrator and heat exchanger design also allows the solar energy to be used to convert zinc from zinc oxide without using a hydrocarbon compound to isolate the oxygen atom from recombining with the zinc.

IAUS Turbine Eliminates Need for Boiler- IAUS'S solar thermal collectors can easily work with either a traditional steam turbine, or with IAUS'S new, proprietary turbine. IAUS'S proprietary turbine steam cycle does not need an expensive, high-maintenance boiler. Instead IAUS'S solar collector system can feed the super-heated water directly into IAUS'S turbine.

IAUS'S solar power technology successfully operates without a boiler or pressure vessel because it utilizes a unique, bladeless turbine design developed by IAUS to drive the electric generator. IAUS'S turbine runs on both high quality and low quality steam with a bi-phase flow capability. Unlike traditional turbines, the high-temperature water does not need to pass through an expansion tank to flash to steam prior to IAUS'S turbine. Instead, IAUS'S bladeless propulsion turbine can run directly on super-heated, high-pressure water.   The expansion or phase change (flashing) from water to steam happens right at the nozzle of IAUS'S turbine.

In a conventional power plant, the water is boiled and flashed to steam in a large, high-pressure tank called an expansion tank. The steam is then sent through a series of super-heating stages. The expansion tank and steam channels are large pressurized vessels that make up the boiler and must be regularly certified. If something goes wrong with this traditional power plant boiler system, it can explode like a bomb. Each weld must be routinely X-Rayed and the entire system continuously monitored with sophisticated and expensive equipment to ensure safety and the output of high-quality steam.

IAUS's system does not need an expensive and sophisticated boiler like this. Instead IAUS's turbine uses a series of smaller, high-pressure tubing, which is much safer, less expensive and easier to manage; and, it makes the Balance of Plant (BOP) steam production and monitoring equipment less complicated. These are significant advantages over traditional boiler systems required by conventional turbines.

 Propulsion Turbine- As previously mentioned IAUS'S solar collector system can operate with either a traditional high-end steam turbine or IAUS'S own proprietary steam turbine. There are many advantages to IAUS'S unique turbine. Rather than relying on turbine blades to spin the turbine cylinder, IAUS's Propulsion Turbine is designed to turn the cylinder without blades. IAUS'S turbine efficiencies are very similar to expensive, high-end, multi-stage turbines; however, IAUS'S turbine is low-cost and operates minus most of the expensive surrounding components and maintenance issues.

9
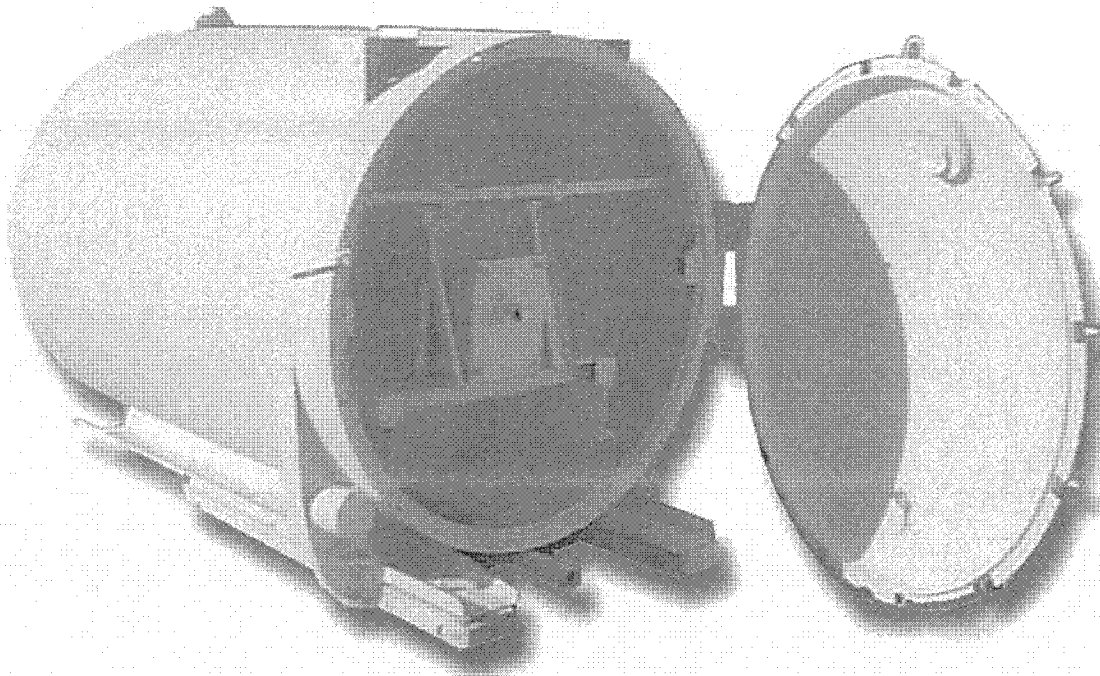
(Figure 5: IAUS bladeless propulsion turbine)

10
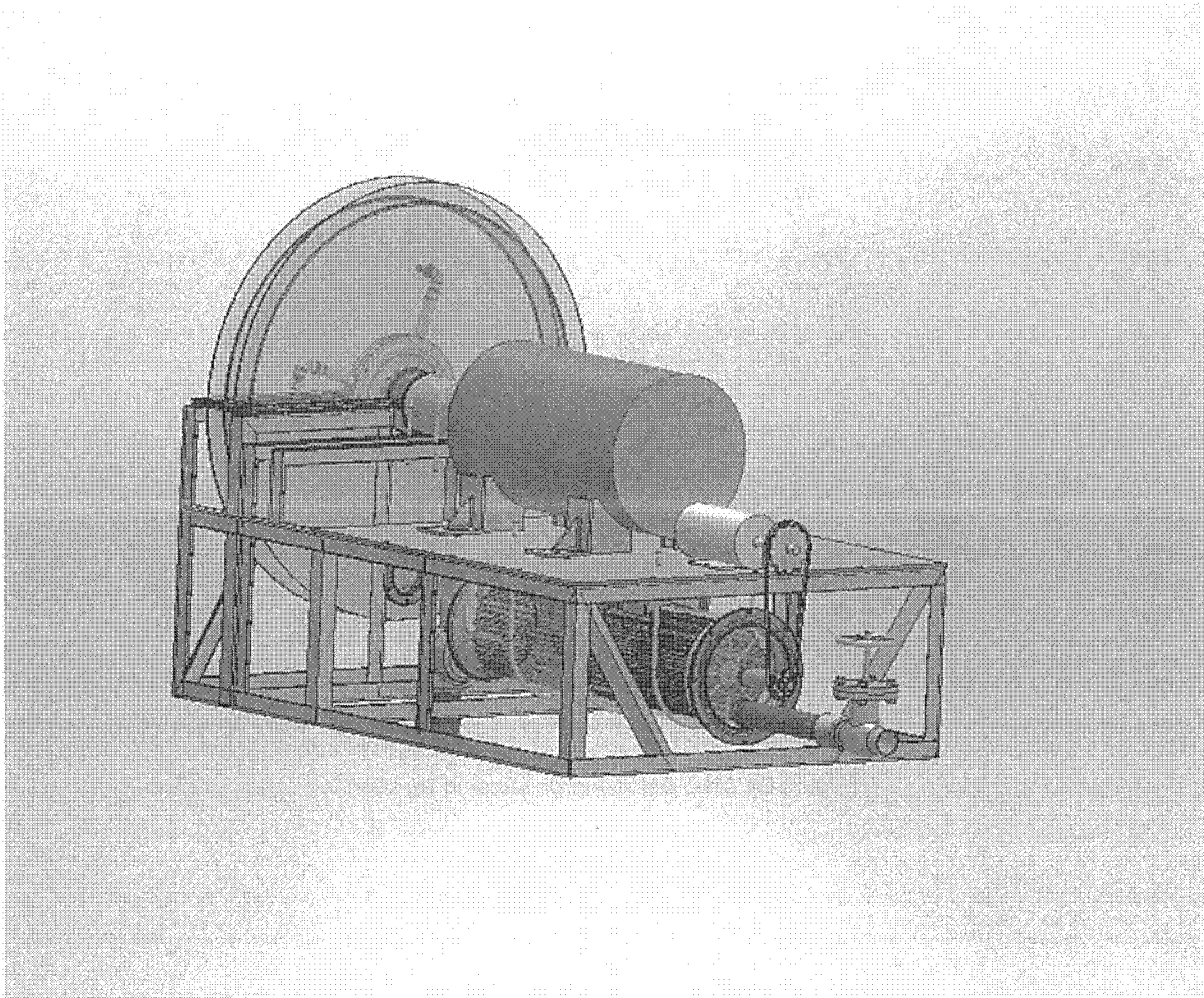
(IAUS's bladeless turbine)

Traditional turbine performance relies upon the environment within its blade chambers. Super-heated, high velocity steam particles are continuously striking the titanium turbine blades to turn the shaft. If steam condenses on the blades, a sharp drop in efficiency and damage to the turbine can result. Traditional multi-stage turbines require dry, high-quality steam.

IAUS's new turbine is structurally unaffected by low quality steam. It blows the energy away from its components instead of on them to turn the shaft. It is smaller than traditional turbines, less expensive, and requires very little maintenance. Unlike traditional turbines, IAUS's turbine can operate without corrosion or system failure on both high quality and low quality steam.

11
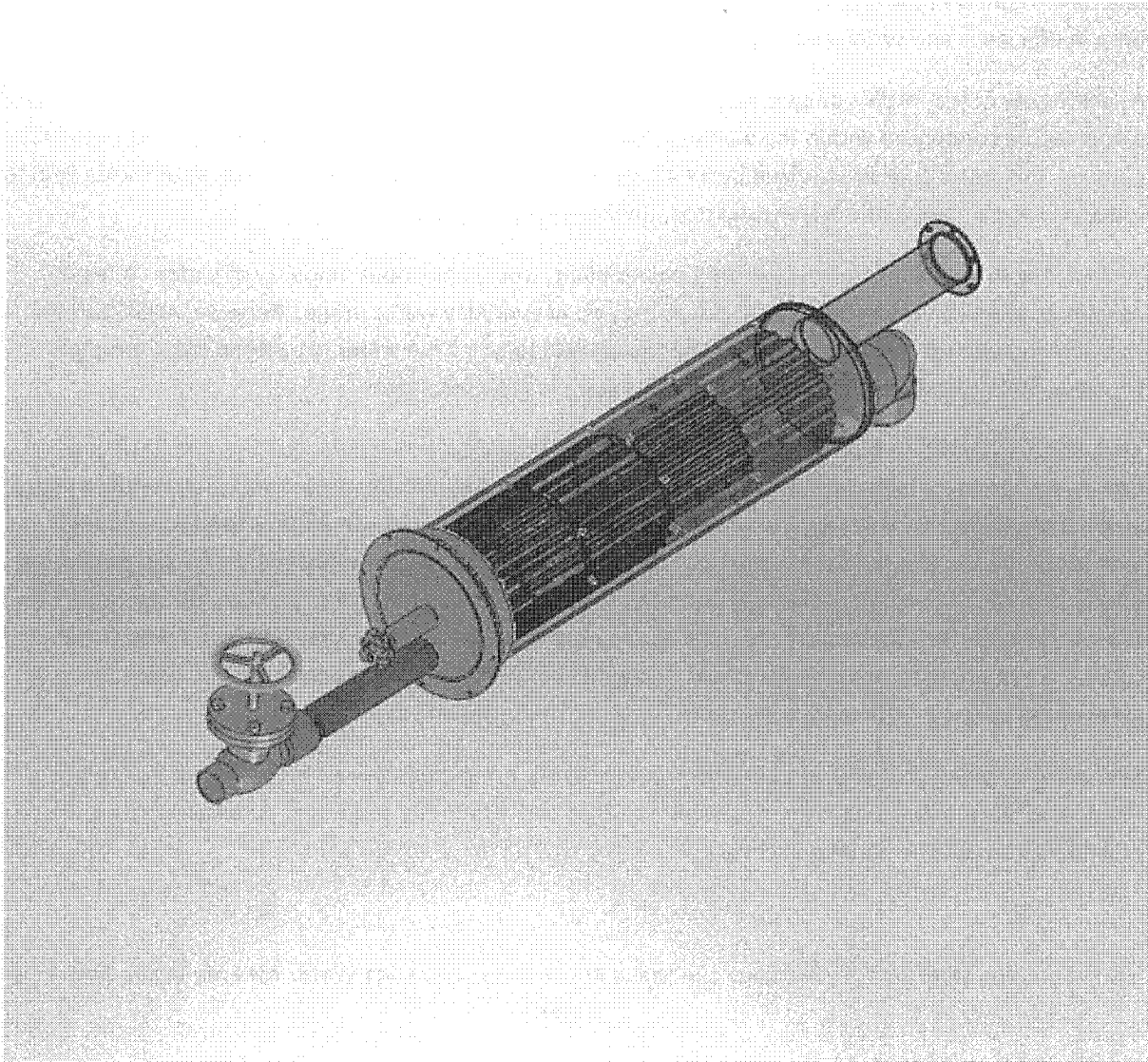
(Figure 5.1 this is the new heat exchanger that recovers the steam from the turbine)

Cooling Towers- Because of the unique nature of IAUS's turbine, the actual working chamber of the

12

turbine can be used as both a direct heat-exchanger and water recovery system on the condensing side. This increases the efficiency and lowers the sophistication and cost of a dry cooling tower. IAUS's system can recycle virtually all of the water used in the process of power production instead of being wasted into the atmosphere like with wet cooling towers that are typically used in the condensing cycle of a traditional power plant.

Cooling towers are a critical component of traditional turbines that help maintain a sophisticated delicate balance. These towers cool the steam exiting the turbine, creating a vacuum. The towers must maintain a consistent low temperature otherwise the traditional turbine potentially faces both a sharp drop in efficiency and serious damage.

As previously noted, IAUS's unique turbine has no blades to corrode, therefore, the expended steam and water can be condensed within the working chamber of the turbine using a simple air-cooled recovery system. This water is re-pressurized by a high-pressure pump and re-circulated through the solar field to repeat the cycle. Very little water is wasted, unlike wet cooling towers.

Wet cooling towers, at a typical coal-fired power plant, waste enormous amounts of water. A family consumes as much water using electricity as they do in everyday water usage. Because IAUS'S turbine can operate without traditional wet cooling towers and recycles the water in a closed loop, it is perfect for areas of the Southwest where water conservation is very important.

Also, because IAUS'S turbine does not require such a delicate balance on the cooling side, IAUS power plants can operate a highly efficient co-generation cycle. The excess heat that is normally wasted in the production of electricity at a typical power plant can instead be put to some other use in conjunction with IAUS's power plants. The thermal and electrical load can easily be adjusted up or down depending upon the need, to best utilize the heat byproduct from the power plant. Putting the heat byproduct to use can increase the efficiency of the plant from approximately 20% up to nearly 70%. A traditional turbine is a poor design for co-generation. It creates difficult BOP consequences including the accelerated corrosion of the turbine itself.

Salt water or brackish water or polluted water recovery using bladeless turbine- In addition to not using water to cool the steam the new IAUS's turbine can also purify salt water, brackish water and or polluted water at little additional costs.

IAUS Solar Breakthrough Technology can Make Fresh Water from Sea Water for Free While Powering a City

Unlike photovoltaic (PV) solar panels, IAUS's new solar breakthrough technology can utilize waste heat to desalinate sea water for free. Waste heat is a byproduct of IAUS's solar power process as it produces electricity for the grid. Due to the unique design of IAUS's patented turbine, it utilizes a technique called

13

vapor compression in the heat recovery process. Vapor compression is becoming a widely-used means for distilling water.

Utilizing the waste heat from an IAUS solar field to produce fresh drinking water increases the overall efficiency of the system to nearly 70% peak power production without a significant increase to the price. Fresh water has become a serious global issue and is predicted to be more perilous than forecasts of current energy issues—both are daunting without renewable energy advancements. In some parts of the world, fresh water is already becoming equal or more expensive to obtain than fuel.

Currently, desalinating sea water costs approximately $800-$1600 per acre foot of water. This price is about 10-20 times greater than the cost a typical farmer currently pays per acre foot to irrigate his crops. In coastal areas around the globe an IAUS solar plant could produce electricity from the sun at an economical price, whereupon the utility company could sell the power to citizens--while at the same time--desalinating water as a waste byproduct for free.

IAUS solar desalination gives IAUS's product a unique edge over other technologies in coastal areas wherein fresh water is becoming a problem due to inland populated areas growing. This ability can greatly help inland communities as well. Some project that the State of Utah will exhaust its Colorado River water shares by the year 2020. Southern Nevada has long been attempting to increase its water shares from the same river. If Southern California coastal cities that are somewhat dependent upon the Colorado River were to utilize an IAUS solar desalination plant—more water shares could be available for Utah, Southern Nevada and others.

Electric Generator- IAUS'S turbine can turn either an induction or synchronized generator to produce AC power that is thereupon connected to the grid through a simple, inexpensive cut-off switch. A traditional turbine drives a synchronized generator and requires a very expensive, instantaneous cut-off switch control mechanism. This is another reason the BOP system for a traditional turbine is very sophisticated. If the supply steam is inadvertently reduced, the grid can turn the electric generator into a motor pulling for more steam supply than is available like a vacuum whereupon the turbine blades will cavitate, potentially causing them to shatter out the chamber like an explosion. This is extremely dangerous.

IAUS's bladeless turbine presents no such danger. The instantaneous shut-off mechanism in the BOP system for IAUS's turbine is not critical to the same degree and is therefore a simpler design and much less expensive. IAUS'S less sophisticated BOP controls not only save a great deal of cost in set up, they can also reduce O&M costs by nearly 1-2 cents or more per kWh.

14

IAUS'S turbine can be sized to virtually any generator, big or small and can start and stop instantaneously without any cavitations. This allows IAUS to construct its solar plant in smaller 1MW-10MW segments if desired. The turbines can be staged in and used only when needed, and they can be shut down at night. When using smaller plant segments, if one important component goes down, it doesn't shut down the whole plant. In contrast, a traditional turbine gen set would be a financial, operational and maintenance nightmare in multiple smaller sizes.

Each 1MW-10MW segment is self-contained and independent of the other. A 1 MW segment consists of approximately 20-25 towers that include 80-100 circles of lenses and receivers all powering a single turbine gen set and water recovery system. The IAUS plant design requires approximately 5-6 acres of land for every 1 MW of peak power capacity.

Comparisons to Other Solar Technologies

Photovoltaic (PV)

Currently, PV is the most expensive solar technology available. PV has advantages for very small, remote power needs, however, even if PV manufacturers are able to reduce costs with the prospect of thin-film or nano PV technology it still will not match the low cost and other advantages of IAUS'S system.

Hidden Costs of PV

Flat-Plate Installation- In addition to installed costs, PV has hidden costs. For example, advertised PV installed costs do not include dual-axis tracking systems. Therefore, a flat-plate mounted PV system measured during peak sun to be 1 KW ($7,000) of capacity actually produces nearly 30% less power annually than 1 KW ($1,500) of IAUS'S dual-axis solar technology.

Inverters- PV technologies produce DC power and therefore, require an inverter to covert DC to AC power. Inverters, regardless of how small or large cost about $500 per KW. While the inverter is usually included in the advertised, installed price of a PV system, it has a very limited life-span after which it must be replaced. The life-span for an inverter is roughly about 20 years. IAUS'S solar can produce either AC or DC power; therefore, IAUS'S system doesn't require an inverter which eliminates one of the front-end and back-end costs that come with PV systems.

Panel Replacement- In addition to inverters, PV panels also begin to degrade after 20-30 years and eventually need to be replaced as well. This means that after 30 years, when the equipment should finally be paid off and realizing the full benefits of free energy, the buyer will likely end up paying the entire cost of the solar plant all over again to replace it.

15

IAUS'S dual-axis solar tracking structure is made of steel and will likely hold up for more than 100 years. Also, IAUS'S actual solar panels are made of a material that has been known to last more than 60 years. However, if needed, the cost of panel replacement for an entire IAUS plant is approximately only 15%-20% of the original cost. The cost to replace the PV system after 20-30 years is virtually 100% of the original cost, which is literally repurchasing the entire plant all over again.

Maintenance Logistics- PV is more suited for residential installations than for utility-scale power plants. In fact, the U.S. Department of Energy has determined that solar thermal technology (not PV) is the most reliable solar power for utility scale power plants. While residential installations have benefits (especially in remote areas outside of the grid), they present different challenges. For example, a 100 MW utility scale solar power plant will power about 50,000 homes from a single location. Installation, part replacement, adjustment, maintenance, etc. can be done in one place. On the other hand, 50,000 homes with PV systems are like scattering 50,000 randomly located miniature power plants all over the map that also include remote locations for installation, part replacement, maintenance etc. Travel time becomes a significant cost, not to mention that each installation site is unique.

Energy Storage- PV systems can only store energy using batteries. Batteries are extremely expensive (about $600/kWh of storage) and have a very short life of about 5 years. Since IAUS'S system runs exclusively on heat, it can operate both as a hybrid power plant using other heat sources in addition to the sun such as biomass, natural gas, etc., or, it can store heat in a heat sink for continued operation after the sun has set. Unlike batteries, heat sinks are inexpensive (about $30/kWh of storage) and a properly designed heat sink will last virtually a lifetime.

Unlike IAUS'S technology, PV systems do not utilize the sun's heat. Since much of the sun's energy is heat, this energy is entirely wasted on PV systems. The heat byproduct from IAUS'S system after producing electricity can be utilized for a list of important uses- manufacturing and refining processes, desalination, heat storage, etc. When this heat is put to use, IAUS'S solar energy efficiency is improved again to more than 3-4 times the efficiency of PV systems.

Manufacturing- Currently, IAUS can produce approximately 350 MW of panels per year. It would cost a solar PV manufacturing company approximately $800 million to duplicate IAUS'S current annual production capacity. Within six months, IAUS can increase its annual capacity to 1,000 MW. Within a year, IAUS can increase its annual capacity to 2,000-4,000 MW. This annual solar panel production capacity would cost a PV manufacturing company a little more than $4 billion. To put IAUS'S production capabilities into perspective, one of the current leaders in PV manufacturing has an annual production capacity of 120 MW.

Environmentally Friendly- IAUS'S solar technology is also 100% recyclable. Today's PV systems using silicone are not.

Solar Thermal Mirrors

Mirrors Require Tighter Tolerances- Solar thermal mirror technology (also called Concentrated Solar Power (CSP)) has been around for decades (e.g. solar dishes, troughs, heliostats). IAUS'S technology is

16

also a CSP system, and therefore, it operates under similar thermal dynamic principles. However, IAUS does not use expensive mirrors. Therefore, IAUS'S panels refract the sun's rays instead of reflect. The error ratio of reflecting the solar rays from a mirror to its target is four times greater than refracting the rays like IAUS'S system does. Therefore, mirror-based CSP support trusses, hinges and tracking systems require significantly tighter tolerances than IAUS's to maintain focus and remain correctly dialed in.

Shadowing Effect of Mirror Receivers- Also, since IAUS'S receiver is behind its panels instead of in front like mirror-based CSPs, it is far less expensive, easier to manufacture and install, and casts no shadow on the panels. IAUS has a smaller insulated receiver with only one flat side exposed to the concentrated focal point, yet it still maintains a greater surface area ratio between focal point size and target than mirror-based CSPs. This minimizes the possibility of the sun's rays missing the receiver. Attempting to increase the ratio between the focal point size and surface area on a mirror-based CSP system in order to minimize losses and increase efficiency would require a larger receiver and a larger receiver would block more incoming sunlight to the mirrors.

Maintenance Issues of Traditional Turbine- The lowest cost, mirror-based CSP systems use a traditional steam cycle to turn a conventional, bladed steam turbine and generator. As mentioned above, IAUS'S steam cycle does not require large expansion tanks to superheat the steam; it does not require water-cooled cooling towers to condense the steam; and it does not require the expensive and sophisticated monitoring devices for BOP due to the rugged durability of IAUS'S turbine under extreme environmental shifts.

The absence of both an expansion tank, traditional turbine and cooling towers not only significantly reduces the overall cost of equipment and installation, but also reduces daily operations and maintenance costs which translate into a lower wholesale price for electricity per kWh produced.

Not Much Room for Price Reduction- After decades of development, current mirror-based CSPs have streamlined down to what appears to a bare minimum cost without many more areas, if any, to cut prices. Each additional refinement or advancement to today's mirror-based CSPs from here on out will likely have an inconsequential impact on lowering the price. IAUS expects to be less than half of the cost of today's CSP technologies, with room to strip down more costs in the future.

CSP Manufacturing Capacity- Manufacturing capacity is a very limiting factor with CSP technology. Most CSP technology companies have a lower annual production capacity than PV manufacturing companies.

<p align="center">**Status of IAUS'S Solar Technology**</p>

IAUS is poised to enter the market in full production with its commercialized product this year. IAUS has already successfully completed a mass-production test run of approximately 2 MW of IAUS solar panels. The dual-axis tracking structure has been constructed and designed for mass-production as well. IAUS'S proprietary software that controls the dual-axis tracking mechanisms has been completed. IAUS'S proprietary controls follow the sun, monitor wind-speed, and measure the sun's energy per square meter. Several generations of the turbine have been designed and tested.

17
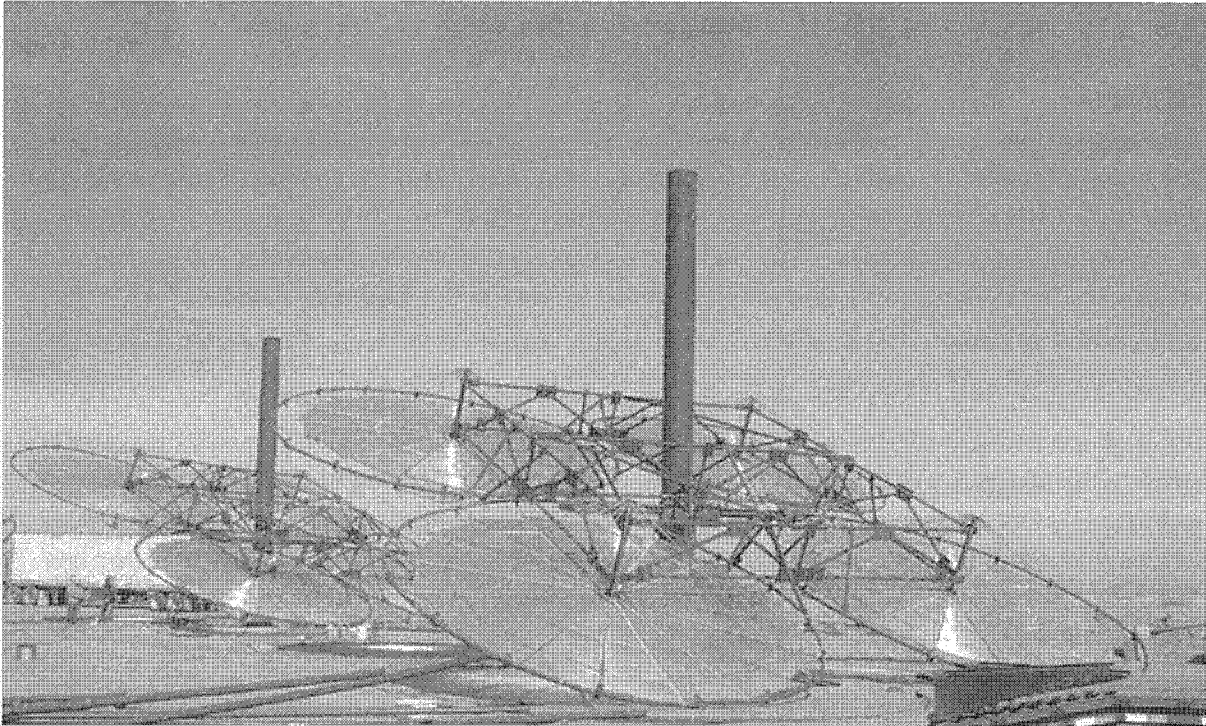
(Figure 6: IAUS solar field under construction)

18
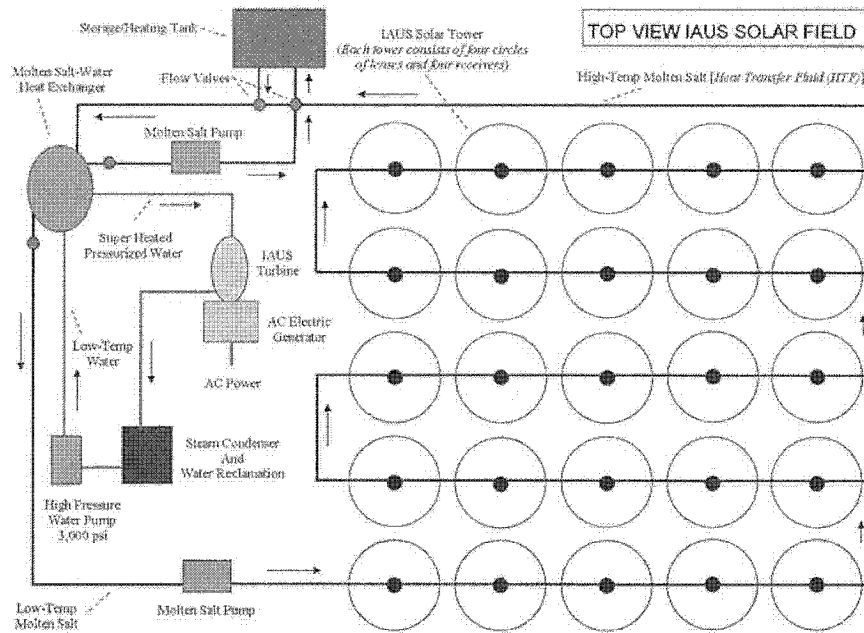
IAUS Technical Overview

Introduction

Concentrated solar power (CSP) technologies focus the sun's heat and convert it into usable energy such as electricity. After more than 20 years of continuous operation, CSP is not considered an experimental technology. Extensive long-term data has been collected from various CSP technologies, to both identify and quantify the definitive factors that affect the annual solar-to-electric efficiencies and economics of a utility-scale CSP plant under actual, real-world circumstances. In one extremely detailed study by the U.S. National Renewable Energy Laboratory (NREL), scientists Sargent and Lundy concluded "that CSP technology is a proven technology for energy production."

Having developed several generations of its unique CSP technology, IAUS is familiar with the material and construction costs of its equipment. Based upon the revolutionary low cost of its new product, IAUS estimated that its proprietary CSP technology needs to reach only a 5% net annual solar-to-electricity efficiency to match the dollar for dollar cost of the currently lowest priced competing CSP technology available. This 5% efficiency benchmark is a reasonable target to reach, being more than 60% below industry standard.

The following report is not intended to detail the low cost of IAUS's unique breakthrough CSP technology, but rather to discuss its overall efficiency based upon independent review. This material addresses the specific scientific data supporting that IAUS's CSP technology achieves an annual solar-to-electric efficiency of nearly 24%- a number that far surpasses its minimum 5% necessary to compete.

As noted, the independent field data covering CSP technologies is extensive. The real affects of dust, transient clouds, parasitic load, energy loss through pipe insulation, etc. are well documented. Enough parallels exist between IAUS's CSP technology and other CSP technologies that the net annual solar-to-electric efficiency of IAUS's technology can be accurately determined by both superimposing common characteristics between IAUS's system and current CSP systems, and isolating and verifying the efficiencies in areas that differ.

IAUS's CSP technology and traditional CSP technologies have a number of differences such as structural design, system controls, operations and management (O&M), as well as others, but in areas that affect the overall net efficiency, there are only two noteworthy differences- the IAUS Propulsion Turbine and Solar Panels. In the thermal-dynamic design of IAUS's CSP system, these two are the only components that have such unique design divergences that numbers from other CSP studies would not necessarily apply. Therefore, this report focuses on the efficiency of both the IAUS turbine and panel design in the form of independent expert review. By combining these numbers with data from other CSP studies compatible to IAUS's CSP system, the annual net solar-to-electric efficiency can be accurately determined and verified.

Note-- In the following section, the third party reviews (both of the IAUS Solar Panels and Turbine) included in this report list the background of the experts and their respective scientific reviews only. No names have been included in this draft for proprietary purposes.

IAUS Solar Panel

The following independent review of IAUS's solar panel efficiency and performance was conducted by a master physicist who is an expert in optical engineering. IAUS's third party optics expert has 50 years of experience in the field of optics, 39 of which were with a leading international electronics corporation where he designed Fresnel lenses and lenticular lenses for projection TVs. He also designed asymmetrical, aspheric lenses for color CRT manufacturing and developed an electrophotographic process to make color CRTs. He is responsible for 20 patents assigned to the above mentioned international electronics corporation.

Evaluation and Overview of the Design Philosophy of IAUS's Solar Panel

This paper will give a brief overview of the design philosophy of IAUS's large Fresnel lens designed for solar energy use. The collection and concentration of sunlight and using the power obtained from the heat to generate electricity is an important goal in man's desires to provide clean virtually inexhaustible power from the sun.

The sunlight falling on earth has a power density of 1,366 watts / sq. meter. At sea level this power density is about 1,000 watts / sq. meter due to atmospheric absorption and scattering. To collect and produce significant amounts of electrical power, large collectors are required. Most people are probably familiar with magnifying lenses and as children may have used them for concentrating sunlight, burning paper, ants or their fingers. A ray tracing made for a small lens is shown in Fig. 1. The source of rays is far away so the incoming rays are essentially parallel.
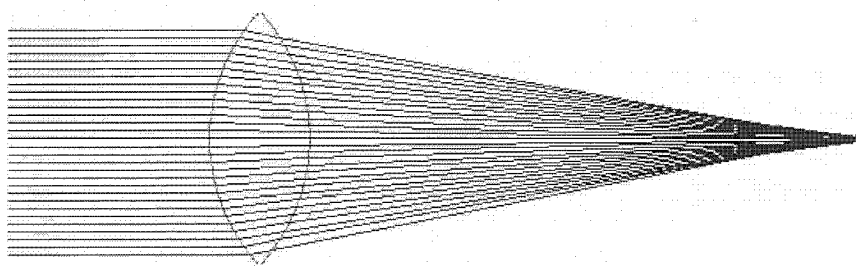

Fig. 1

The focal length is fairly long in the tracing above. The f-number is approximately 2.2 A lens of this design would mean that the target is far removed from the lens. For the large diameter lenses we want to consider, large structures would be needed to support the lens. It is desirable to have a lens with a short focal length.

20

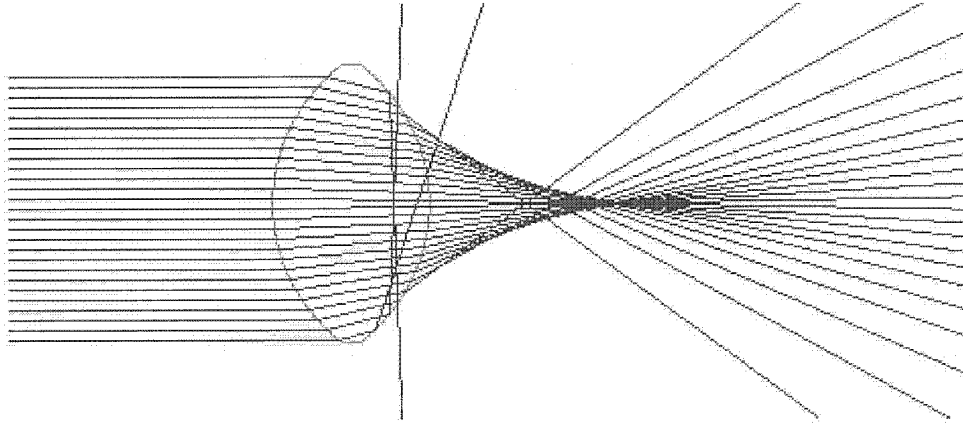A lens of a much shorter focal length is shown in Fig. 2. The f-number is approximately 1.0

Fig. 2

In the case of this low f-number lens, we get a short focal length however there is much aberration which smears out the rays in the focal region and there are some rays undergoing total internal reflection (TIR). We will come to these problems later.

To extend the principle of the magnifying lens to large collection areas requires a very large lens. The thickness in the center of the lens in Fig. 2 is a large percentage (60%) of the lens diameter. Considering the size of the collectors desired in this project, 436 inch (36.33 feet) diameter, a lens made in the proportions to the one in Fig. 2 would have a thickness of about 262 inches. This would be a very expensive and heavy lens. Another concern would be how much sunlight would be lost traversing such a thick piece of material.

A way around this problem is to put facets in a surface so that the refractive power still exists to bend light but the thickness does not build up. See Fig. 3. Light houses need such a lens working pretty much opposite to our needs. The rays from a nearly point source of light are collected and made to project to a parallel beam of light for a long distance. In 1823 the first lens of this type of construction used for a

21

light house and was used and credited to Augustin-Jean Fresnel.
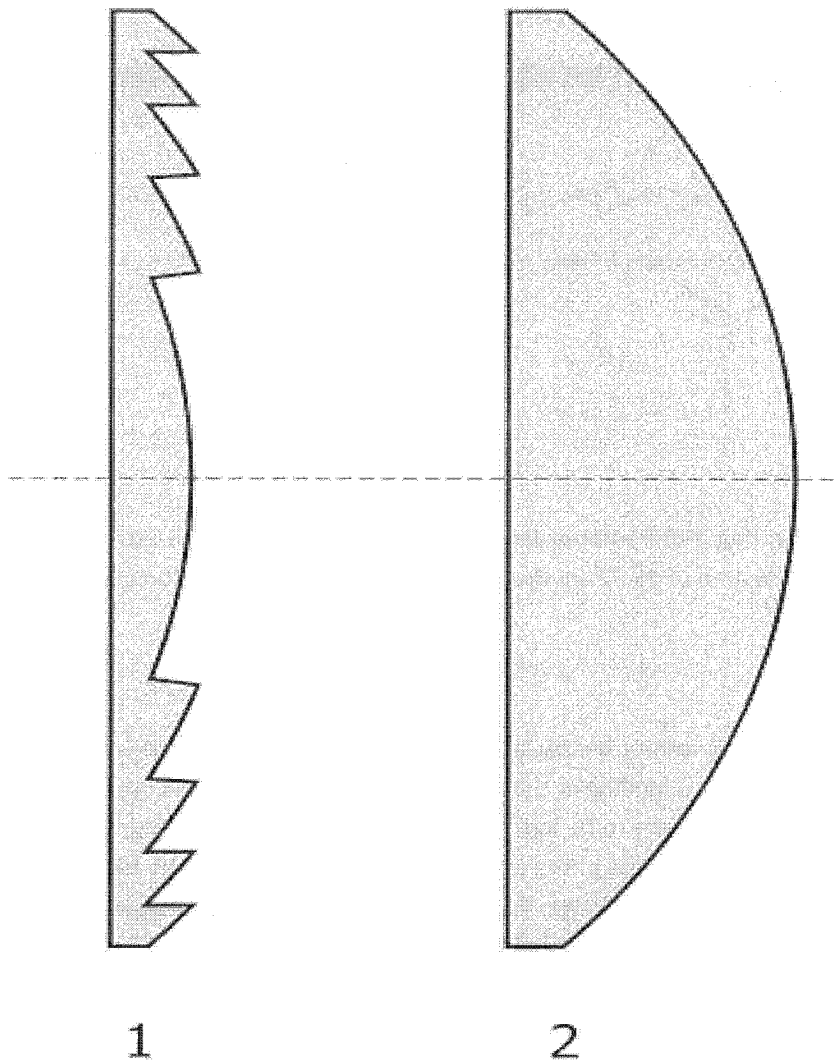

1   2

Fig. 3 (Wikipedia)

As can be readily seen, much less material is used to construct the Fresnel lens than the conventional lens. In addition the slope of each facet can be controlled so that spherical aberration is eliminated. This is of concern when designing a short focal length lens was evidenced in Fig. 2.

A number of items needed to be considered in the design of IAUS's Fresnel lens for solar energy collection.

Below is a drawing identifying some of IAUS's Fresnel lens components.

22
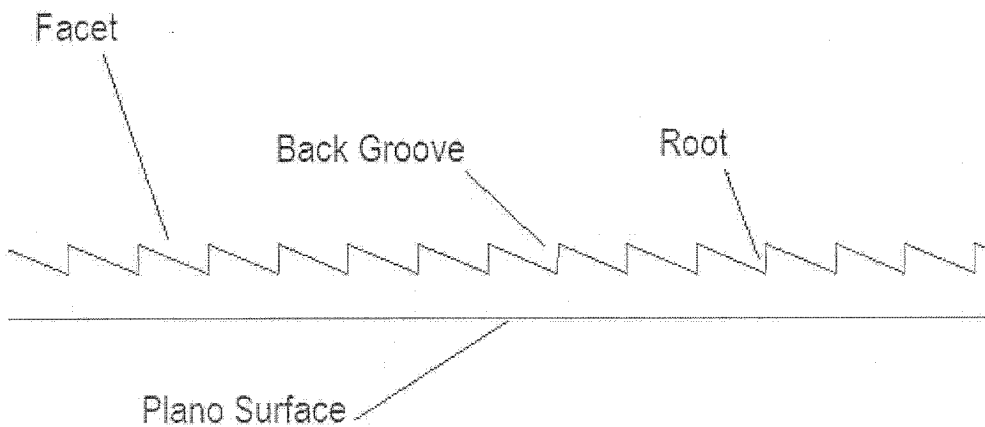
1   **Diameter.** The power generating requirements determine the diameter. For this project, the lens diameter of 436 inches has an area of 96.32 sq. meters and has a 100 kW collection capacity potential.

2   **Groove pitch.** The groove spacing cannot be too large as the facet angle will not be correct across a long facet and produce errors in rays landing in the focal plane. If the groove spacing is too small, diffraction effects will start to cause rays to be lost from the main rays and a loss of efficiency will occur. In the present design, the thickness of the lens was to be kept small. As the facet angles changed from the center of the lens to the edge, this meant that the groove pitch had to change as a function of position in order to provide enough thickness at the bottoms of the grooves to hold the lens together. Near the center of the lens the facet angles are small and the pitch of the grooves can be relatively large, but away from the center of the lens, the facet angles increase in order to refract light more to reach the focal plane. The steeper facet slopes thus cut into the lens at a steeper angle and cannot be extended as far as the facets near the lens center. At the outer edges of the lens the facet angles were steep.
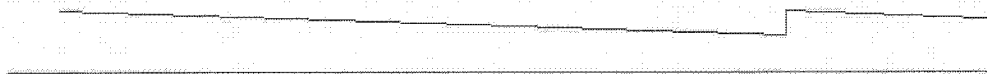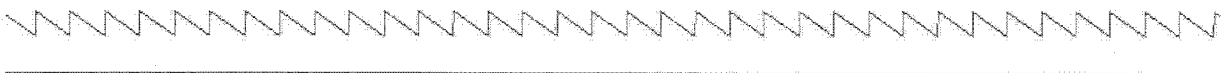

7 Inches from the center.

23
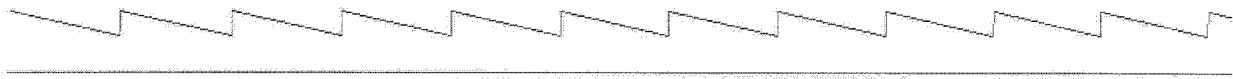
50 Inches from the center.
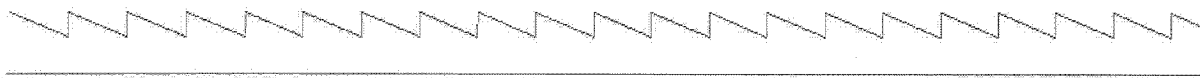
100 Inches from the center.

204 Inches from the center.

3 **Groove Back Angle.** For the purposes of releasing the lens from the mold developed by IAUS, the back angles of the grooves had to provide relief. For this lens 0.5 degrees of relief was used in the design.

5 **Groove Root Radius** The tool used to cut the grooves in the mold is not infinitely sharp and so a finite radius was used in the design. This was taken into account in the ray traces. Eventually a very small radius was used (0.0001 inch) so that it had negligible effect on the efficiency of the lens.

6 **Focal length.** The shortest focal length possible is desired for mounting space. However refractive and reflective properties of optical materials and the laws of refraction and reflection limit just how small the focal length can be. The following plots show the Fresnel reflection effects due to rays passing through mediums of different indices of refraction. Fresnel also has reflection equations associated with his name. The equations below represent the amount of reflection for waves with components parallel to the plane of incidence and perpendicular to the plane of incidence.

Fresnel Reflection Co-efficients

24

$$Rs = (\sin(\theta2 - \theta1) / (\sin(\theta2 + \theta1)) \wedge 2$$

$$Rp = (\tan(\theta2 - \theta1) / \tan(\theta2 + \theta1)) \wedge 2$$

Where:

Rs = reflection component perpendicular to the plane of incidence.

Rp = reflection component parallel to the plane of incidence.

$\theta1$ = angle of incidence.

$\theta2$ = angle of refraction.
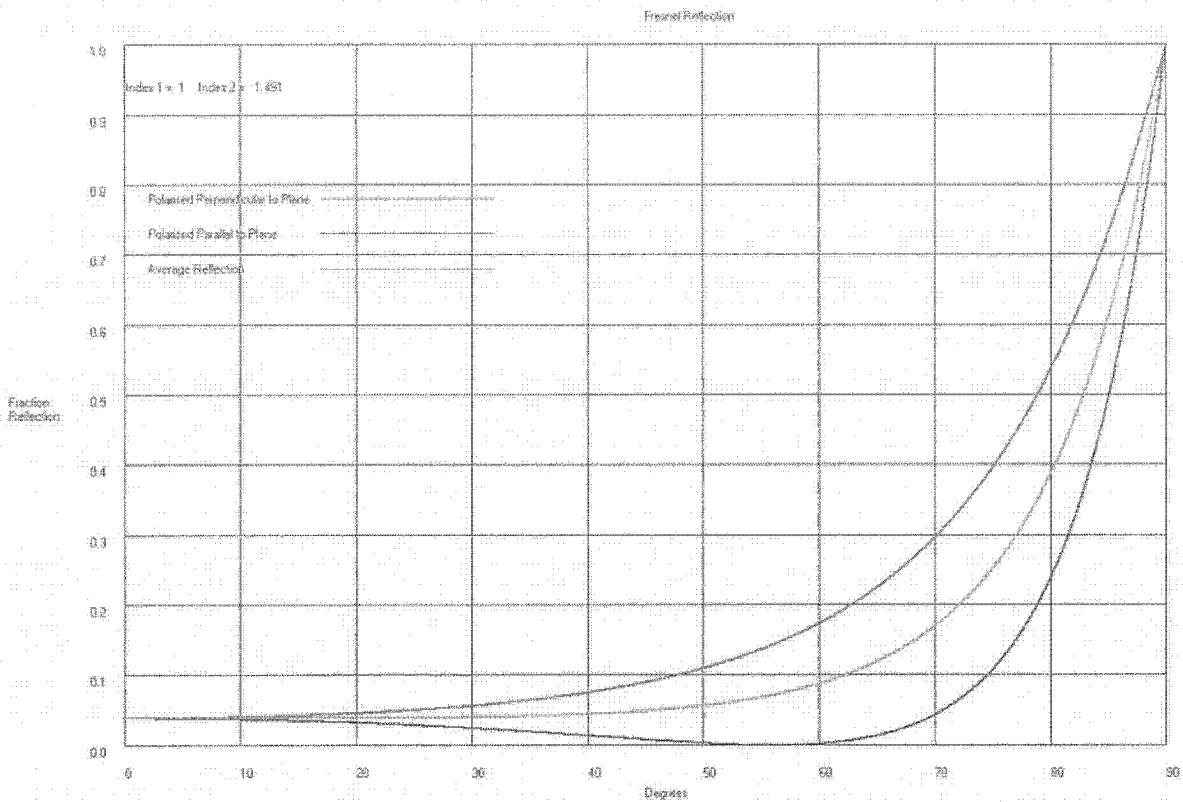
R. W. Ditchburn: Light, 1963 PP 14.8

Fig. 4

25

The above plot shows the reflection of the parallel and perpendicular components of light vectors undergoing reflection when entering a material of index 1.491 from air. We see that there is about 4% reflection for light entering at zero degrees incidence and that the reflection increases as the angle of incidence increases. At 60 degrees the average value reflected is about 8%. Thus for best efficiency the design should minimize the angle of incidence. However this means that the focal length would be large which is not desirable.

In the case where the rays leave a high index material into air the situation is much different. At angles of about 42 degrees incident all of the rays are reflected, this is referred to as total internal reflection (TIR) which means that no rays in those areas would get to the focal point target. We can see that below:
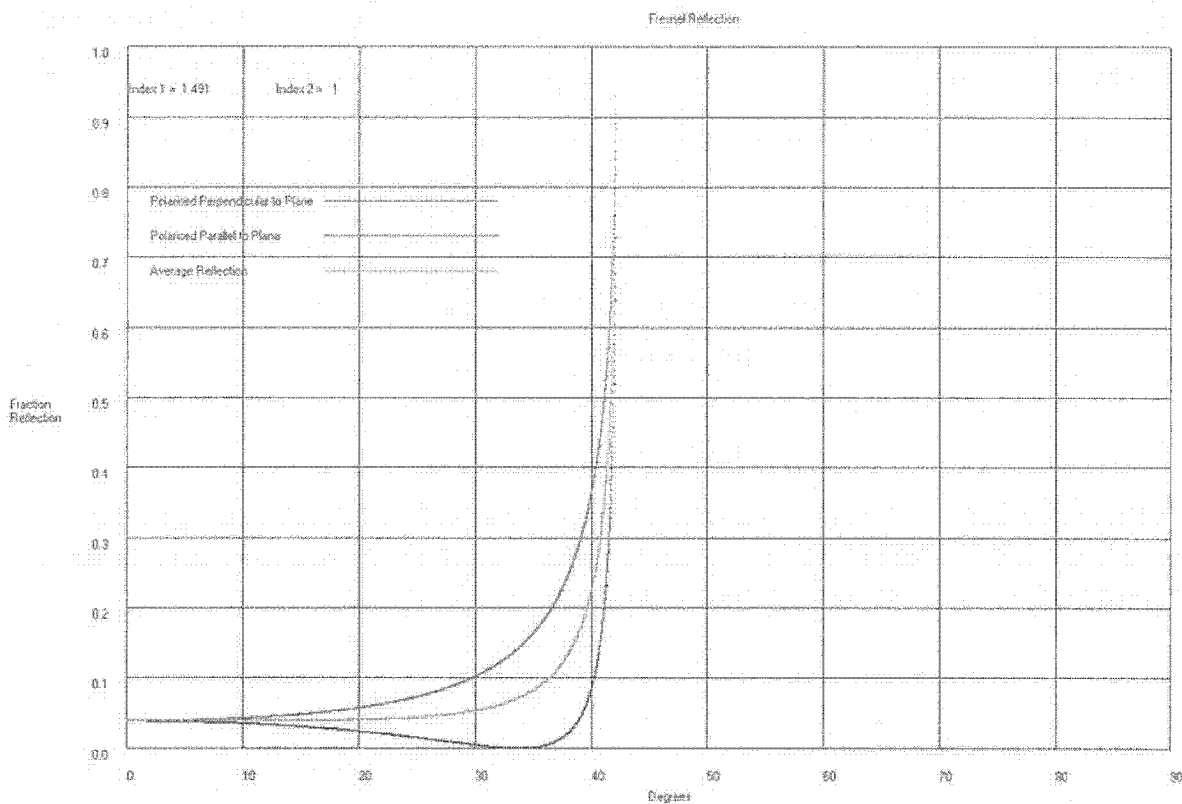
Fig. 5

The ray tracing program uses the Fresnel reflection co-efficients in the ray tracing so that the efficiency of designs can be evaluated. Many designs were considered in order to determine the best comprise focal length and efficiency. Fig. 6 shows the efficiency fall off from center to edge across short focal length lenses.

Fresnel
Efficiency vs Radius of Used Area
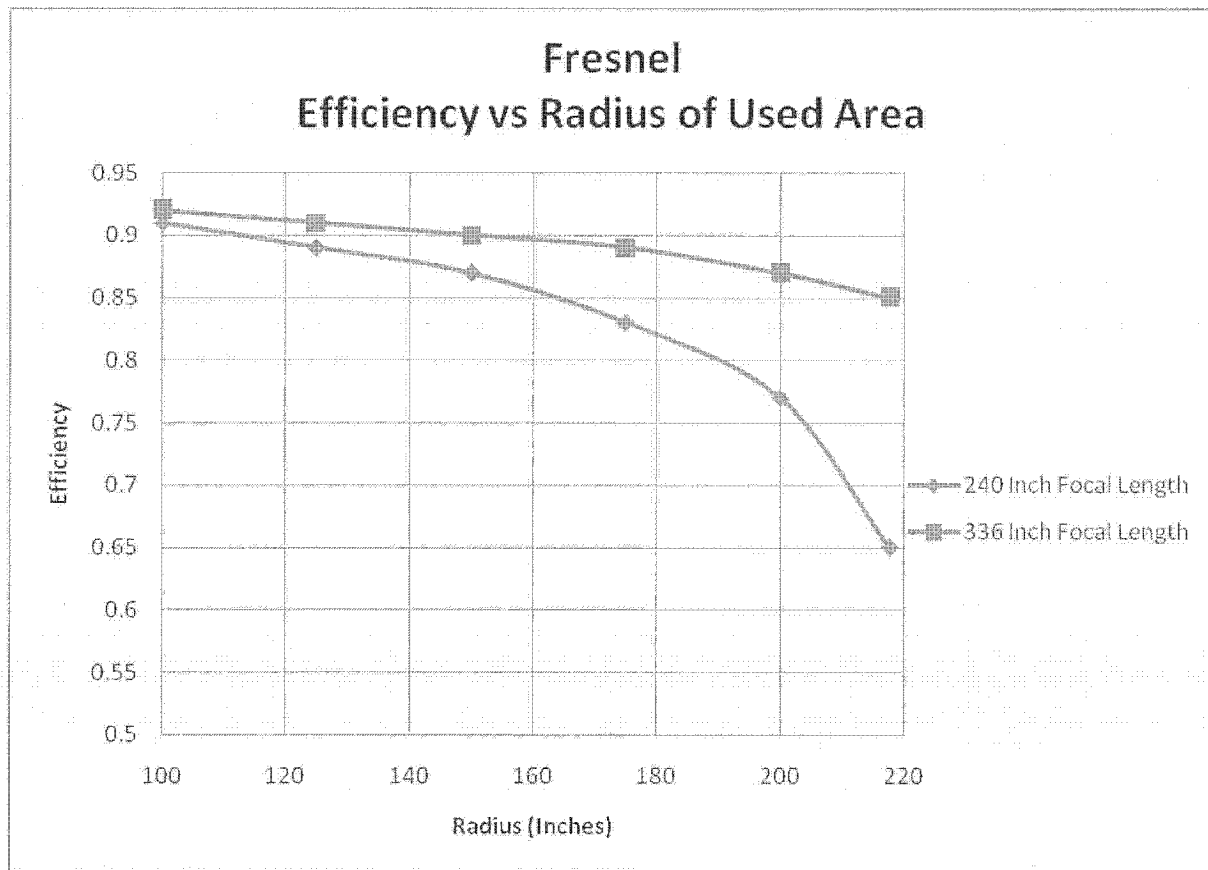
Fig. 6

Ray traces were made (Fig 7) to determine the efficiency of various focal length lens designs. The longest focal lengths had the highest efficiencies but to keep the size of the overall optical system to a reasonable value a focal length of 450 inches was chosen for the final design.

27

Fresnel (206" Radius)
Efficiency vs. Focal Length
Sun Ray Trace
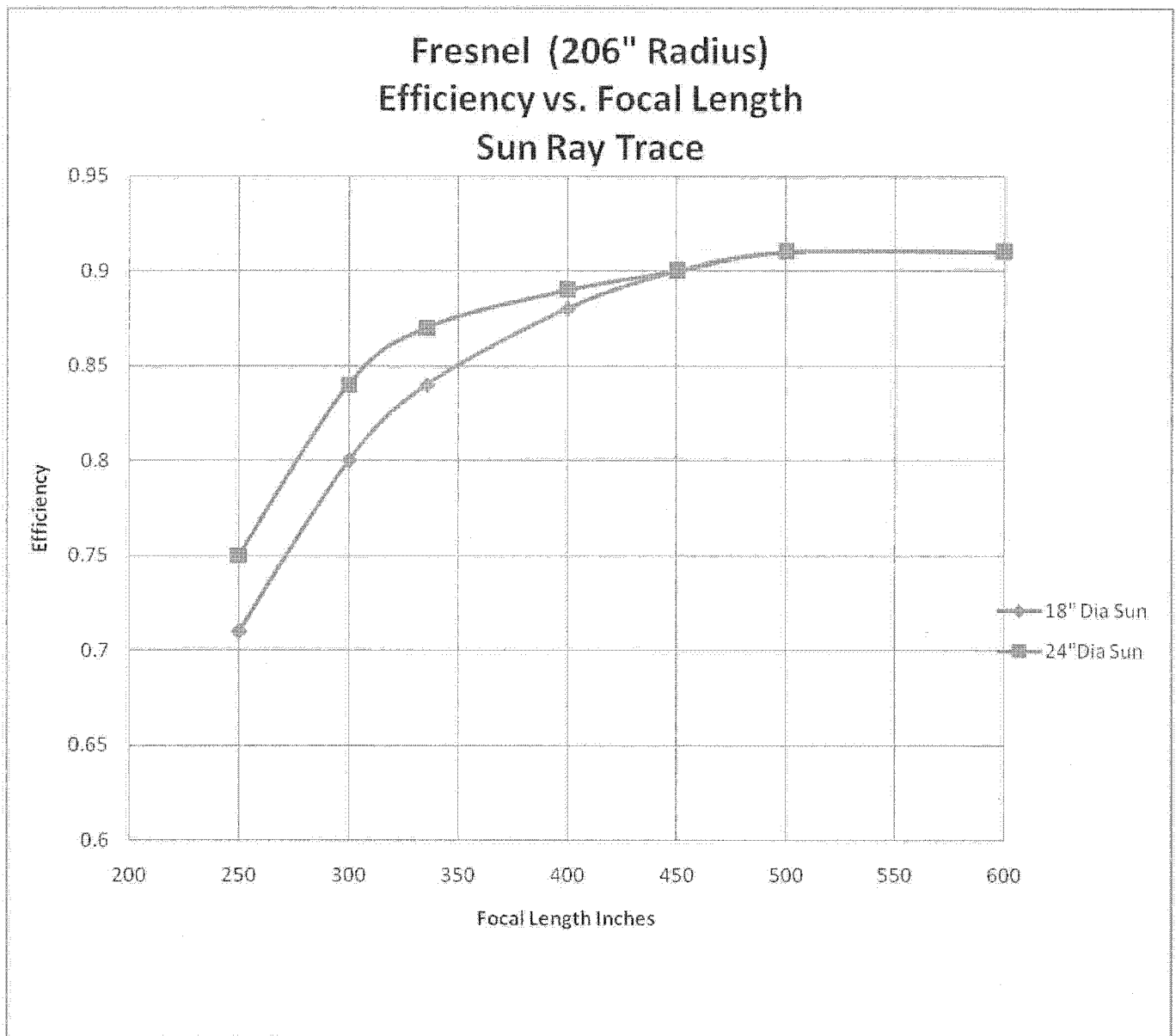
Fig. 7

We find from the plot that only about a 2% gain in efficiency would be obtained by going to a longer focal length than 450 inches.

7   Ray Tracing.   In the ray tracing program, rays were initiated to simulate rays coming from the sun. Rays were sent to the lens at various angles to simulate the finite size of the sun (angular extent of about 0.52 degrees). The well known Snell's law was used in the ray tracing program to calculate the angle of refraction when a ray met a boundary.

28

$$N1*\sin(\theta 1) = N2*\sin(\theta 2)$$

Where N1 and N2 are the indices of refraction of the media in which the ray traverses and θ1 and θ2 are the angles of incidence and refraction at the boundary of media of the ray passing from medium one to medium two.

The solar spectrum contains energy at many wavelengths. In Fig. 8 we see that most of the power is contained in the 300 to 1,000 nm range. At the shorter wavelengths the earth's atmosphere blocks most of the power and many plastic materials do not transmit the rays.
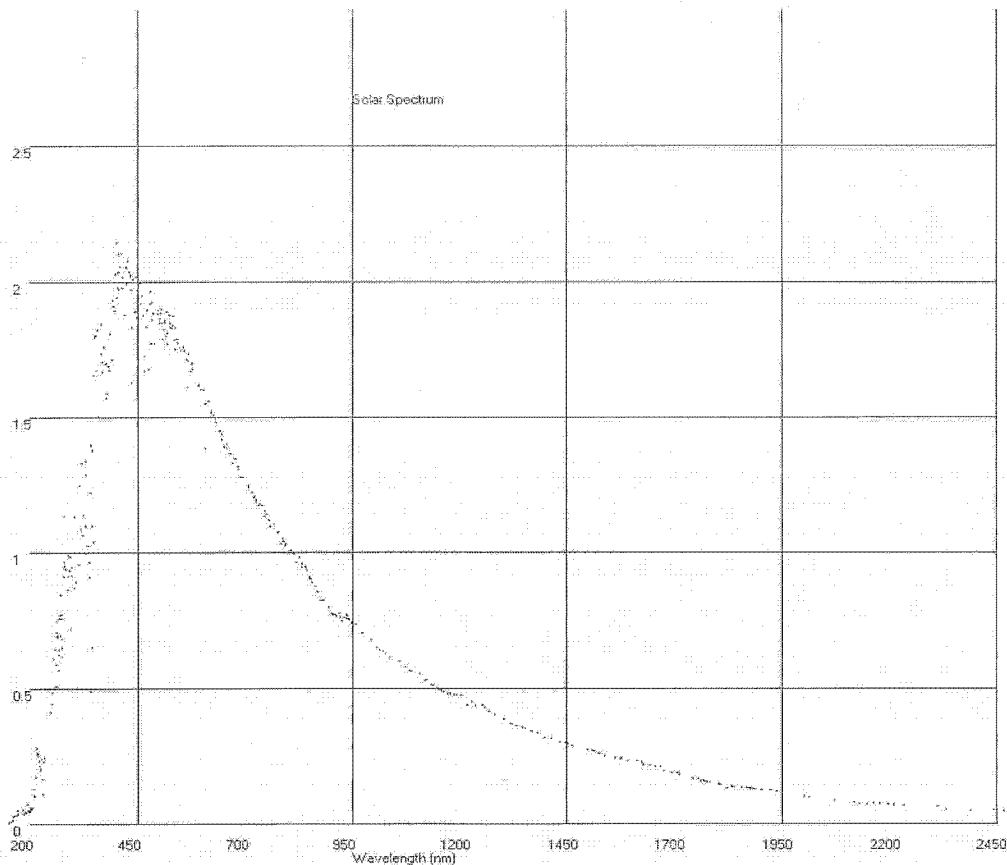
Fig. 8

PMMA which is used as the material to make IAUS's Fresnel lens has an index of refraction which varies as wavelength (humidity and temperature also affect the index of refraction but this was not considered in ray tracing). This means that rays of different wavelengths will bend different angles as they pass through the boundaries of the material. In ray tracing two different values of index of refraction were used, representing different parts of the solar spectrum, namely 1.491 and 1.482 which represent wavelengths of roughly 400 nm and 800 nm in the solar spectrum. This brackets the power range of

29

sunlight at the earth's surface. As a result of the 5 solar locations and the 2 wavelengths and the spacing of the rays traced, 0.001 inch, over 2,000,000 rays were traced for each analysis run.

Fig. 9 shows a detail of a ray tracing made with much fewer rays than normally run to better show what each ray is doing. In this section the rays are coming in from above and sent towards the right towards the Fresnel lens axis.

Fig. 9

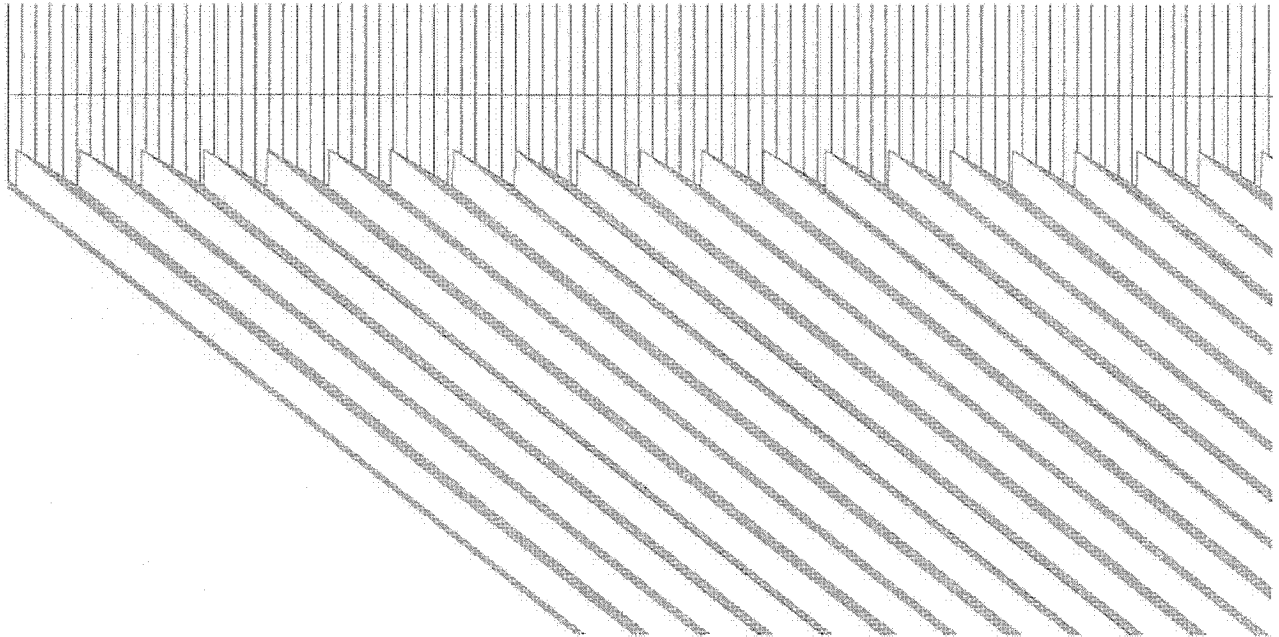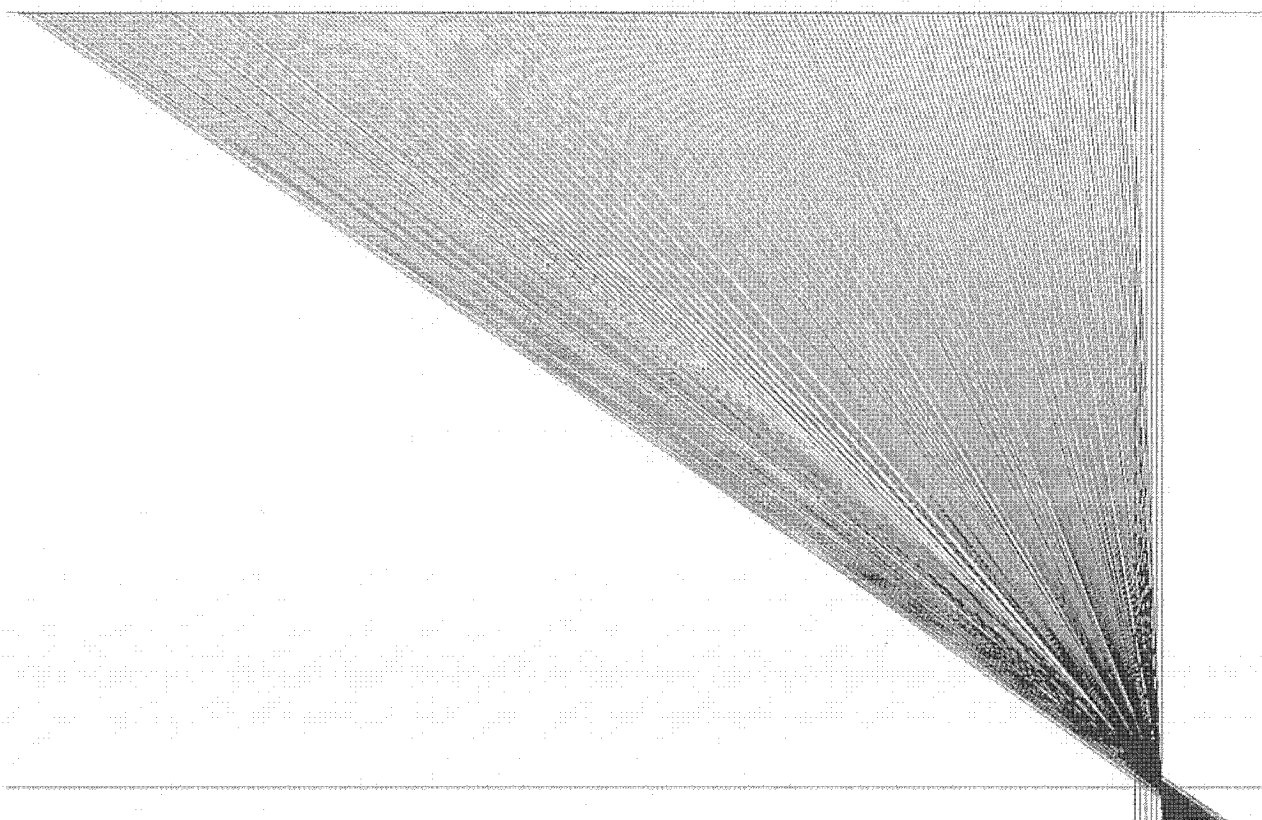In Fig. 10 the overall redirection and focusing of the left half of the Fresnel lens is shown.

30

Fig. 10

In Fig. 11 the zone near the focal plane is shown in detail. The center 12 inch diameter of IAUS's lens does not have any facets and so there are some rays that come straight down to the target without focusing.

31
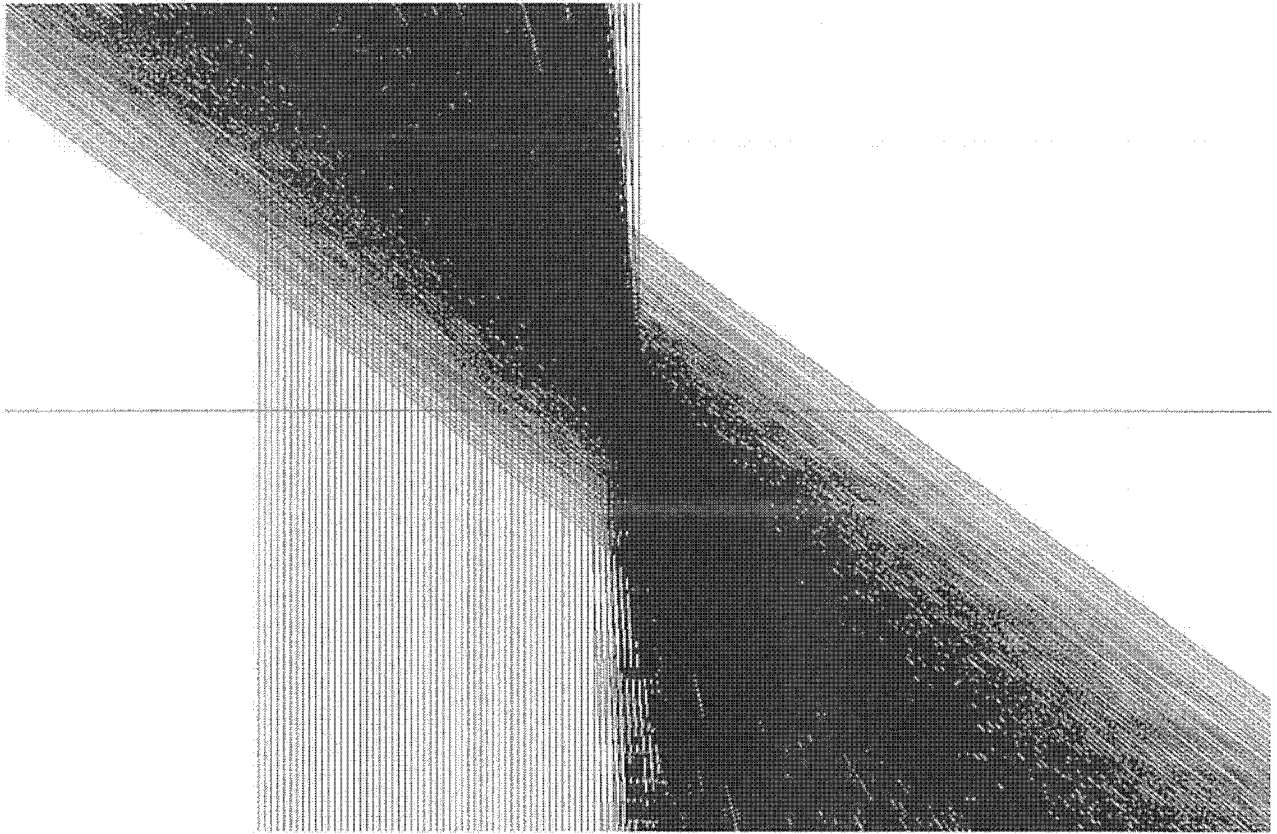
Fig. 10

Only the rays focused from the left half of the lens are traced here. Again the center of IAUS's lens does not have any facets and the rays from the center are shown coming straight down without focusing.

Temperature calculations across the focal plane were made based on a thermodynamic equation given in book by Leutz and Susuki "Nonimaging Fresnel Lenses, Design and Performance of Solar Concentrators". On page 20 the following equation is given:

$$Tmax = T \, sun * (C / Cmax) \wedge .25$$

The maximum temperature in Kelvins is equal to the temperature of the sun (5777K) times the fourth root of the Fresnel concentrator divided by the maximum possible concentration (43,400). This equation was used for temperature calculations; however the temperatures seem a little high. I contacted one of the authors of the book (Leutz) and he also felt it gave temperatures higher than gotten in practice but did not have an explanation. Perhaps the exact geometry, emissivity and thermal conductivity of the actual target do not match the theoretical model assumed by the thermodynamic equation. In any case the temperature distribution is proportional to the rays traced and their intensity at the target.

The computer program generates a report file so that all the parameters used and the results of the ray tracing are tabulated. Below is a report for the 450 inch focal length design.

32

"DesignFresnel 1.217 12-21-08"

"Todays Date","01-12-2009"

" "

"Fresnel Design Data *****************"

" "

"Units   ","Inches"

"Fresnel Focal Length   ",450

"Constant Groove Depth   ",.04

"Groove Root Radius   ",.0001

"Fresnel Groove Relief Angle Degrees   ",.5

"Fresnel Thickness   ",.1

"Fresnel Start Radius   ",6

"Fresnel End Radius   ",218

"Fresnel Design Index of Refraction   ",1.491

"Air Index of Refraction   ",1.000293

"Number of Grooves   ",2299

"Step Size in Angle Calculation (Rad) ",.00002

" "

"Ray Trace Conditions *******************************"

" "

"Rays Traced Nonsequentially"

"Source   ","Sun"

"Number of Source Positions ",5

"Ray Index Traced   ",1.491

"Ray Index Traced   ",1.482

33

"Target Position   ",450

"Ray Starting Position   ",0

"Ray Stop Position   ",206

"Ray Step Value   ",.001

"Number of Rays Traced   ",2060000

"Fraction Passing First Surface   ","0.96"

"Fraction Passing Second Surface (no grooves)","0.00"

"Fraction Passing on Grooves   ","0.91"

"Fraction Passing on Relief Back   ","0.00"

"Fraction Passing in Groove Radius   ","0.00"

" "

"Target Results********************************"

"Number of Target Sizes   ",15

"Target Diameter   ",2,"Fraction of Rays in Diameter   ","0.19"

"Target Diameter   ",4,"Fraction of Rays in Diameter   ","0.44"

"Target Diameter   ",6,"Fraction of Rays in Diameter   ","0.60"

"Target Diameter   ",8,"Fraction of Rays in Diameter   ","0.74"

"Target Diameter   ",10,"Fraction of Rays in Diameter   ","0.79"

"Target Diameter   ",12,"Fraction of Rays in Diameter   ","0.83"

"Target Diameter   ",14,"Fraction of Rays in Diameter   ","0.86"

"Target Diameter   ",16,"Fraction of Rays in Diameter   ","0.88"

"Target Diameter   ",18,"Fraction of Rays in Diameter   ","0.90"

"Target Diameter   ",20,"Fraction of Rays in Diameter   ","0.90"

"Target Diameter   ",22,"Fraction of Rays in Diameter   ","0.90"

"Target Diameter   ",24,"Fraction of Rays in Diameter   ","0.90"

34

"Target Diameter   ",30,"Fraction of Rays in Diameter   ","0.90"

"Target Diameter   ",36,"Fraction of Rays in Diameter   ","0.90"

"Target Diameter   ",1000,"Fraction of Rays in Diameter   ","0.91"

"   "

"Temperature Profile of Target **"

"   "

"Solar Constant Used (watts/meter sq)   ",1000

"Absorbtivity of Target   ",.986

"   "

"Target Diameter ",2,"   Concentration Ratio   ","7,861.7"," Temperature in Disk ","3,069"

"Target Diameter ",4,"   Concentration Ratio   ","4,616.3"," Temperature in Disk ","2,724"

"Target Diameter ",6,"   Concentration Ratio   ","2,806.1"," Temperature in Disk ","2,440"

"Target Diameter ",8,"   Concentration Ratio   ","1,954.5"," Temperature in Disk ","2,255"

"Target Diameter ",10,"   Concentration Ratio   ","1,339.2"," Temperature in Disk ","2,079"

"Target Diameter ",12,"   Concentration Ratio   ","980.1"," Temperature in Disk ","1,945"

"Target Diameter ",14,"   Concentration Ratio   ","745.4"," Temperature in Disk ","1,836"

"Target Diameter ",16,"   Concentration Ratio   ","585.7"," Temperature in Disk ","1,747"

"Target Diameter ",18,"   Concentration Ratio   ","469.4"," Temperature in Disk ","1,669"

"Target Diameter ",20,"   Concentration Ratio   ","383.2"," Temperature in Disk ","1,601"

"Target Diameter ",22,"   Concentration Ratio   ","316.7"," Temperature in Disk ","1,540"

"Target Diameter ",24,"   Concentration Ratio   ","266.1"," Temperature in Disk ","1,488"

"Target Diameter ",30,"   Concentration Ratio   ","170.4"," Temperature in Disk ","1,362"

"Target Diameter ",36,"   Concentration Ratio   ","118.4"," Temperature in Disk ","1,270"

"Target Diameter ",1000,"   Concentration Ratio   ","0.2"," Temperature in Disk ","484"

"   "

35

"Target Position   ",0,"   Temperature Kelvins   ","3,786"

"Target Position   ",1,"   Temperature Kelvins   ","3,155"

"Target Position   ",2,"   Temperature Kelvins   ","2,547"

"Target Position   ",3,"   Temperature Kelvins   ","2,305"

"Target Position   ",4,"   Temperature Kelvins   ","1,765"

"Target Position   ",5,"   Temperature Kelvins   ","1,625"

"Target Position   ",6,"   Temperature Kelvins   ","1,458"

"Target Position   ",7,"   Temperature Kelvins   ","1,346"

"Target Position   ",8,"   Temperature Kelvins   ","1,177"

"Target Position   ",9,"   Temperature Kelvins   ","1,037"

"Target Position   ",10,"   Temperature Kelvins   ","493"

"Target Position   ",11,"   Temperature Kelvins   ","532"

"Target Position   ",12,"   Temperature Kelvins   ","549"

"Target Position   ",13,"   Temperature Kelvins   ","569"

"Target Position   ",14,"   Temperature Kelvins   ","575"

"Target Position   ",15,"   Temperature Kelvins   ","579"

"Target Position   ",16,"   Temperature Kelvins   ","585"

"Target Position   ",17,"   Temperature Kelvins   ","579"

"Target Position   ",18,"   Temperature Kelvins   ","573"

"Target Position   ",19,"   Temperature Kelvins   ","566"

"Target Position   ",20,"   Temperature Kelvins   ","553"

"Target Position   ",21,"   Temperature Kelvins   ","553"

"Target Position   ",22,"   Temperature Kelvins   ","532"

"Target Position   ",23,"   Temperature Kelvins   ","525"

"Target Position   ",24,"   Temperature Kelvins   ","504"

36

"Target Position   ",25,"   Temperature Kelvins   ","492"

"Target Position   ",26,"   Temperature Kelvins   ","477"

"Target Position   ",27,"   Temperature Kelvins   ","450"

"Target Position   ",28,"   Temperature Kelvins   ","449"

"Target Position   ",29,"   Temperature Kelvins   ","419"

"Target Position   ",30,"   Temperature Kelvins   ","416"

"Target Position   ",31,"   Temperature Kelvins   ","386"

"Target Position   ",32,"   Temperature Kelvins   ","378"

"Target Position   ",33,"   Temperature Kelvins   ","373"

"Target Position   ",34,"   Temperature Kelvins   ","372"

"Target Position   ",35,"   Temperature Kelvins   ","376"

"Target Position   ",36,"   Temperature Kelvins   ","381"

"Target Position   ",37,"   Temperature Kelvins   ","375"

"Target Position   ",38,"   Temperature Kelvins   ","377"

"Target Position   ",39,"   Temperature Kelvins   ","369"

"Target Position   ",40,"   Temperature Kelvins   ","384"

"Target Position   ",41,"   Temperature Kelvins   ","385"

"Target Position   ",42,"   Temperature Kelvins   ","375"

"Target Position   ",43,"   Temperature Kelvins   ","382"

"Target Position   ",44,"   Temperature Kelvins   ","388"

"Target Position   ",45,"   Temperature Kelvins   ","371"

"Target Position   ",46,"   Temperature Kelvins   ","380"

"Target Position   ",47,"   Temperature Kelvins   ","377"

"Target Position   ",48,"   Temperature Kelvins   ","364"

"Target Position   ",49,"   Temperature Kelvins   ","372"

37

IAUS Propulsion Turbine

The following independent review of IAUS's Propulsion Turbine efficiency and performance was conducted by two specialized engineering firms. The lead engineer from Engineering Company #1 is an expert in combustion stability, liquid rocket engine performance and injector design, and laser diagnostics. He received his B.S. degree in Chemical Engineering from M.I.T., his M.S. degree in Mechanical Engineering from the University of Miami, and his Ph.D. in Mechanical Engineering from U.C. Berkley.   The second engineer from Company #1 is an expert in system optimization, mechanical and fluid systems analysis, liquid rocket engine performance, solid and gel propellant performance, and component design. He received his B.S. degree in Mechanical Engineering from V.M.I. and his M.S. degree in Nuclear Engineering from M.I.T. Engineering Company #1 is specialized in propulsion technology and has worked with government agencies such as NASA, U.S. Missile Defense Agency, U.S. Air Force, and Office of Secretary of Defense.

In addition to other experience, the lead engineer for Engineering Company #2 is an expert in structural loads prediction, stress analysis and mechanical design; structural dynamics including rotating machinery and vibration; the use of finite element methods and computer analysis programs to solve stress and dynamic loading problems, including composite structures; and probabilistic and statistical design, analysis and data reduction. He received his B.S., M.S., and Ph.D. degrees in Mechanical Engineering from U.C. Davis. His Ph.D. dissertation was on practical nonlinear simulation of rotating machinery dynamics with application to turbine blade rubbing.

The new IAUS propulsion turbine offers several advantages over traditional turbines. The steam cycle starts at the nozzle. This eliminates the boiler steam generation cycle. The boiler steam generation cycle required by traditional turbines increase the cost of the system, increases maintenance, and reduces efficiency.   Also because the turbine exit temperature can be higher than traditional turbines it uses air to condense the steam back to water which eliminates the need for costly cooling towers and the use of water used to cool the traditional turbine exit steam temperature. Again this reduces cost by eliminating costly cooling towers and water requirements.

IAUS has developed special heat exchangers both for heating the water and for cooling the water. These heat exchangers do not need the complicated traditional piping system now used in traditional steam turbines. The new heat exchanger design eliminates the piping used in the traditional heat exchangers. This eliminates most of the maintenance required.

They new heat exchangers developed by IAUS also will allow for very inexpensive biomass energy systems. The turbine can be used to produce electrical energy from a variety of sources. The new heat exchangers can make all forms of fuel more efficient and make biomass competitive with coal and other fossil fuels.

One of the main reasons why biomass fuels are not competitive with fossil fuels in the high cost involved with transporting these types of fuels. By using the new IAUS turbine the turbines can be

made smaller and therefore, can be placed close to the biomass supply. This means the where now biomass was not profitable it can be made very profitable and competitive with traditional fuels.

IAUS Propulsion Turbine Evaluation

1. INTRODUCTION

This report is an update to, and supersedes, previous Sierra Engineering Inc (Sierra) reports on the parametric sizing and performance of the International Automated Systems (IAUS) bladeless steam turbine. The major change in methodology for this revision is the definition of system efficiency. Previous reports have considered the turbine as a system rather than as a component. As such, the efficiency was defined as the ratio of output shaft to total available enthalpy drop. The total available enthalpy drop was taken as the difference between the turbine inlet enthalpy and the enthalpy of the steam when expanded isentropically to ambient pressure (14.7 psia). This definition also neglects any energy recovery that may be achieved from subsequent water condensation. The current report treats the turbine as a component in a closed cycle steam system. As such, we are reporting only the efficiency of the turbine to make shaft power from the energy extracted from the steam. The current definition of efficiency is thus:

Turbine Efficiency = Output Shaft Power / (Flow rate x Ideal Enthalpy Drop)

where the ideal enthalpy drop is the difference between the turbine inlet enthalpy and the enthalpy of the steam when expanded isentropically to the nozzle exit pressure. For all designs considered, the nozzle has been sized to expand the steam to 95% quality.

Sierra has developed a first order system analysis tool to evaluate bladeless steam turbine performance and geometry. The tool predicts the required steam flow rate and nozzle radial distance necessary to produce the desired generator output (1 MW). An analytical hydraulic model of the steam flow through the power shaft and turbine supply tubes has been included to assess the system pressure drop. Aerodynamic drag on the turbine rotor disk is also assessed. Basic analytical structural burst and rotordynamic critical speed analysis models of the power shaft and nozzle supply tubes have also been included in the system analysis.

Specific design parameters included in this first-order system design trade include:

- Power level,
- Gear box ratio (or absence of a gear box),
- Turbine rotational speed,
- Nozzle radial position and number of nozzles on the turbine,
- Nozzle supply tube diameter,
- Nozzle design,
- Bearing frictional losses, disc and nozzle aero drag,
- Steam supply conditions, and

39

- Material of fabrication (by specification of allowable stress levels).

A system design trade was conducted for a 1 MW generator. The design trade assumed:

- 3200 psia steam supply pressure
- 1460 R steam supply temperature
- 95% steam quality at the nozzle exit
- 96% generator efficiency
- 1% bearing friction loss
- 1% gear box friction loss (if present, for low gear ratios with one gear mesh)
- No seal frictional loss nor mass leakage through the seals

A cursory design optimization was performed considering the following design parametrics:

- 1800, 3200, and 3600 RPM generator speeds
- 0.5, 1.0, and 2.0 gear box ratios for the 3200 RPM generator
- 4, 6, and 8 exhaust nozzles

2.   CONCLUSIONS

The baseline turbine inlet conditions are 3200 psia inlet pressure and turbine inlet temperature of 1000 F (1460 R). The current design recommendations are:

Generator speed:		3600 RPM
Gear box ratio:	1.0	
Number of exhaust nozzles:		8
Radial nozzle feed tube I.D.:		0.50 inch
Radial nozzle feed tube O.D.:		1.25 inch
Exhaust nozzle radial center line:		26.2 inch
Predicted turbine efficiency:		43.81%

We also recommend the following preliminary characteristics for the system:

- Include bearings on both sides of the turbine disc
- Maximize the number of steam nozzles
- Reduce size of radial supply tubes while keeping the internal pressure drop at a reasonable level (<100 psid)

40

- Avoid using a gear-box despite improved turbine efficiency (+2.5% with 7200 RPM turbine), due to analysis uncertainty and additional cost

Details of the analysis approach, trade space considered and trends are presented in the following sections. A more detailed turbine optimization will require establishment of the following:

1. design limits on the maximum number of nozzles and the potential flow interactions developed between adjacent nozzles;

2. development of a list of acceptable materials for the use of tube and nozzle manifold fabrication;

3. cost limits for component and assembly manufacture, since this may limit material sections;

4. expansion of the fluid property database.

41

3. ANALYSIS TOOLS

System model: Excel based module

Steam properties: ALLPROPS 6/4/96

Nozzle Design: ONC '98

Nozzle performance: TDK '01

Steam circuit hydraulics: Excel based module

Turbine supply tube structural: Excel based module

- Centrifugal and pressure burst
- Rotor critical speed

4. APPROACH

The Excel-based system model was developed to predict the required steam flow rate and overall turbine efficiency as a function of a set of input parameters. This system analysis model is supported by other analysis modules; a system structural module, and a system hydraulics module.

The structural analysis module predicts the required thickness of the nozzle supply tube to withstand pressure and centrifugal forces. The required bearing stiffness is determined to ensure 25% RPM margin from the first rotordynamic critical speed. Rotordynamic analysis assumes bearings are present on each side of the rotor for maximum bearing stiffness effectiveness, i.e. the rotor is not overhung.

The structural analysis assumed the use of AISI 321 stainless steel in the ½-hard condition. This material should provide the minimum strength characteristics needed for prolonged application with high-temperature steam. The material allowable stress analysis was decremented by 10% to provide some degree of margin. Table 1 presents the allowable stress for AISI 321 stainless steel as a function of condition, as well as the design allowable stress used for the present trade study.

Alternate materials of fabrication can be used, however, the allowable strength should be at least equal to the design stress presented above, assuming the mass density is similar to that of a steel alloy. Higher strength materials effectively increase the design factor of safety and are therefore more desirable. Due to the peculiarity that the centrifugal loads (via mass) increase proportionately with increasing supply tube cross section area, a certain minimum strength material is required for a design, i.e. making the tube thicker is not necessarily a design solution. The material must also have low creep and good strength at 1000°F for long periods, as do AISI 321 and 347 stainless steels.

Table 1. Material Allowable and design strength of AISI 321 Stainless Steel.

Material Condition	Allowable Strengths @ 1000F	Design Strength @ 1000F
	(psi)	(psi)
321SS annealed	15860	
321SS 1/4 hard	42090	
321SS 1/2 hard	56730	51057
321SS 3/4 hard	71980	
321SS full hard	83570	

The hydraulic analysis of the turbine divides the system down into seven segments. These segments include:

1. form loss for the supply port to the supply manifold,
2. form loss for the supply manifold to the shaft port(s),
3. form loss for the shaft port(s) to the inner shaft,
4. frictional loss for the flow down the inner shaft,
5. form loss for the inner shaft flow to the nozzle feed lines,
6. frictional loss for the nozzle feed lines, and
7. form loss for the nozzle feed lines to the nozzles.

Current analyses have assumed that the fluid density and viscosity are constant through the flow circuit. Figure 1 provides an illustration identifying these pressure drop elements. Prediction of the form loss for each of the turns is performed in a similar manner. The technique utilized was developed during the late 1960's as part of the NASA program with Aerojet General entitled "Injector Orifice Study – Apollo Service Propulsion System", contract NAS9-6925.
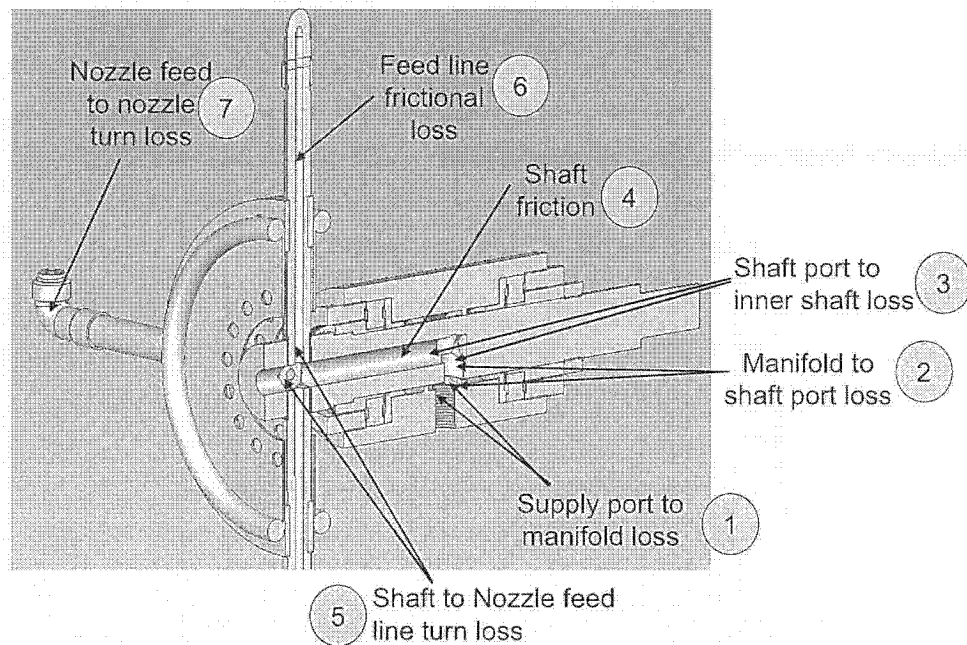
43

Figure 1. Definition of Components in Hydraulic Analysis

The technique provides a method for prediction of the size of the vena contracta at a turn or an area contraction (**Figure 2**). Utilizing the area of the vena contracta a 1-D velocity of the liquid is calculated along with a corresponding dynamic head. The pressure drop associated with this geometric feature (e.g. turn or flow contraction) is then calculated as a sudden expansion from the vena contracta to the local flow area using the standard sudden expansion form loss expression (Figure 3).
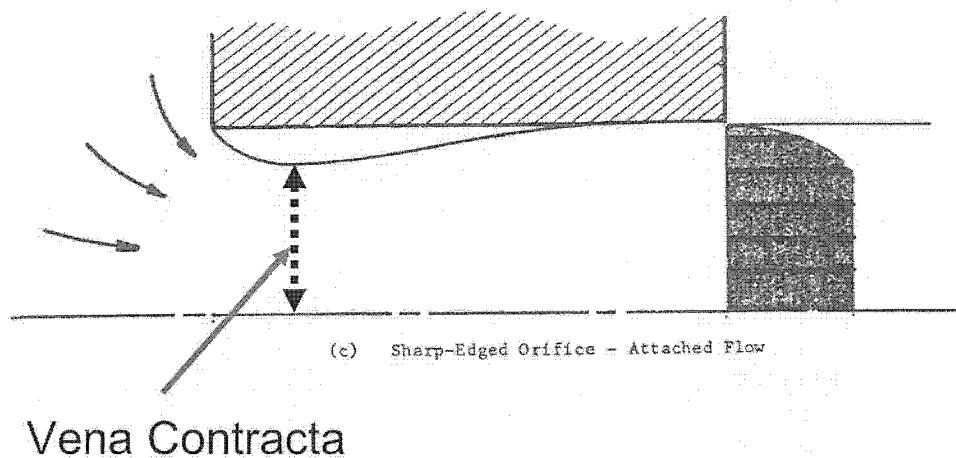

(c)   Sharp-Edged Orifice - Attached Flow

Vena Contracta

Figure 2. Sketch of Vena Contracta at the Entrance of a Sharp Edge Orifice
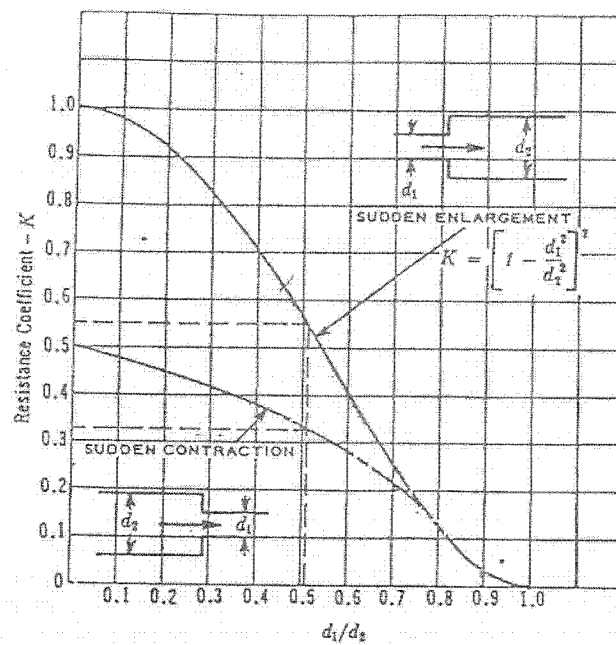
44

Figure 3. Form Loss Factors for Sudden Expansions and Contractions

The frictional pressure drop through the shaft and nozzle supply tubes is predicted using a standard friction factor coefficient correlation with a surface roughness of 32 micro-inches.

45

5.   SYSTEM DESIGN TRADES

Four primary design variables were used during the system design trades - the generator operating speed, gear box ratio, the turbine radius, and the nozzle supply tube internal diameter. For each design trial, the steam pressure drop and required nozzle supply tube thickness were computed to achieve the required output power of 1 MW. With a system balance in place, the turbine efficiency was then estimated.

Figure 4 shows that the turbine efficiency increases with decreasing inlet steam temperature, but increased steam flow is required to achieve the desired power output. It is important to note that the minimum steam inlet temperature is above 760 F; at lower temperatures the nozzle exhaust velocity will not be sonic. Turbine specific power (Shaft Power / Mass Flow) improves with increasing steam inlet temperature. This should result in increased overall cycle efficiency, as reduced flow rates will also reduce pump power. Thus the figure of merit should be turbine specific power and not turbine component efficiency.
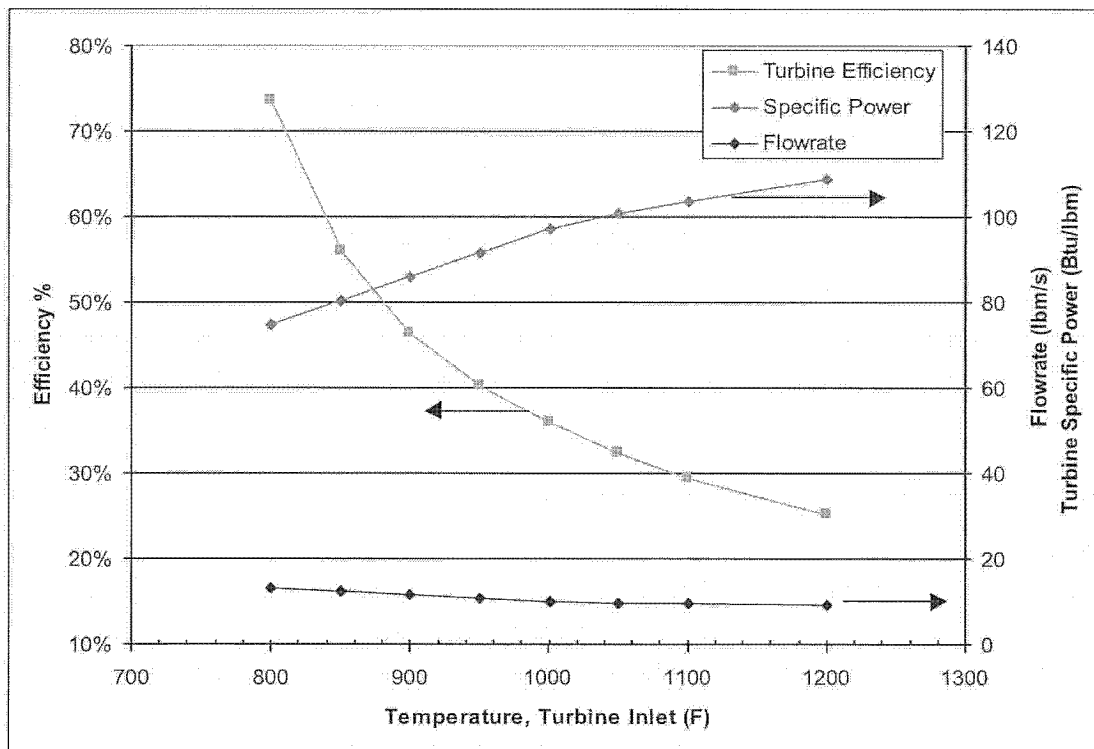

Figure 4. Turbine Efficiency and Flow Rate vs. Inlet Temperature

Figure 5 shows that the nozzle becomes more efficient at extracting enthalpy from the steam as the steam feed temperature increases. This also points to the importance of maintaining high fluid temperatures.
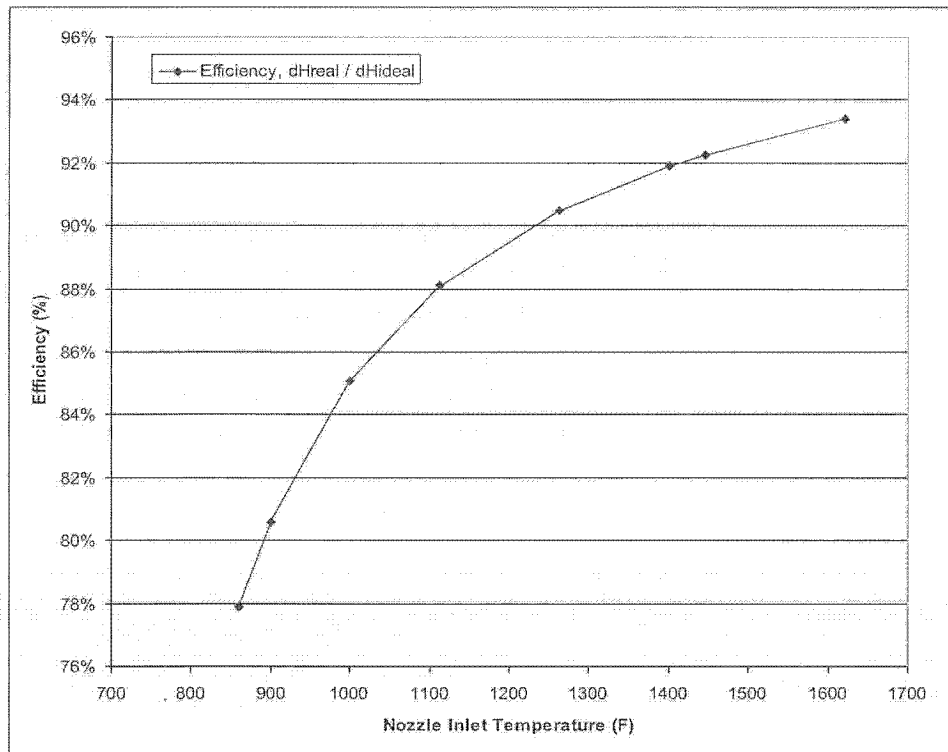
Figure 5. Enthalpy Extraction Efficiency of Nozzle

It should be noted that all efficiency calculations were performed assuming that the turbine is surrounded by dry air at 14.7 psia and 70 F. This selection effects the turbine performance in two ways. First, it defines the fluid that the turbine housing interacts with, producing drag. Second, the ambient pressure acts against the exit area of the turbine nozzle to reduce the delivered thrust. Reducing the surrounding gas to near vacuum conditions will reduce both the surface drag and the thrust loss, resulting in an estimated efficiency improvement from 43% to 52%.

It is certainly desirable to avoid using a gearbox, due to the high cost of an additional precision manufactured element in the system. Eliminating a gear box also permits use of a common induction motor/generator, which runs at constant speed and is low cost. But at this stage, it was necessary to determine whether use of a gearbox provided an improvement in overall turbine efficiency.

Figure 6 presents the summary of the design trade on gear box ratio, assuming 4 equally spaced nozzles. The results of the design trade indicate that an increasing gear box ratio, i.e. a faster turbine relative to the motor, also increases efficiency. A peak turbine efficiency is nearly 4% higher with a gear box ratio of 2:1 (46.1%) than for a similar case without a gear box (4 nozzles with a tube ID of 0.5 inches).

Figure 7 illustrates the impact of gear box ratio and radial tube inside diameter on radial tube outside diameter. The use of a gear box ratio of 2:1 increases the outside diameter to over 2.5 inches. This

47

would seem to be excessive, given the modest increase in turbine efficiency. Therefore, omission of a gearbox is recommended.

Figure 8 presents the predicted turbine efficiency as a function of generator drive speed for a gear box ratio of 1.0 and 4 equally spaced nozzles. These data indicate that there is some benefit of moving toward a higher generator drive speed. However, as shown previously, the higher drive speeds requires a thicker radial nozzle feed tube. A more detailed analysis of the impact of radial nozzle feed tube thickness should be investigated, along with cost and maintenance impacts of using a higher speed generator, should be included in the detailed design optimization.

Figure 9 presents the predicted turbine efficiency as a function of number of exhaust nozzles for a generator drive speed of 3600 RPM and a gear box ratio of 1.0. These data indicate that there is minimal increase in efficiency as the number of nozzles is increased. These data also indicate that there is a small benefit from reducing the internal diameter of the radial feed tubes.

Figure 10 presents the required bearing stiffness as a function of number of exhaust nozzles and the radial tube internal diameter for a gear box ratio of 1.0 and a generator drive speed of 3600 RPM. These bearing stiffness values are readily achievable.

Finally, Figure 11 presents the required radial tube outside diameter as a function of number of exhaust nozzles and tube inside diameter. Tube thickness increases with increased tube inner diameter, but pressure drop decreases. To ensure that these results are reasonable, an effort is required to do some detailed design of the exhaust nozzle manifolds and attachment to the radial feed tubes.

Table 2 and Table 3 present a numerical summary of the analysis results. These results, and the trends discussed above, imply that the best design would make use of the maximum number of steam nozzles allowable, as determined by structural analysis and mechanical design, and the smallest allowable tubes, as limited by steam flow velocities and pressure drop. This implies the need to establish the following design constraints that will be important in subsequent design optimization:

1. design limits on the maximum number of nozzles (the question of where flow interactions develop which may hinder turbine performance needs to be answered),

2. development of a list of acceptable materials for the use of tube and nozzle manifold fabrication (this feeds into the weight of the components and the associated structural sizing), and

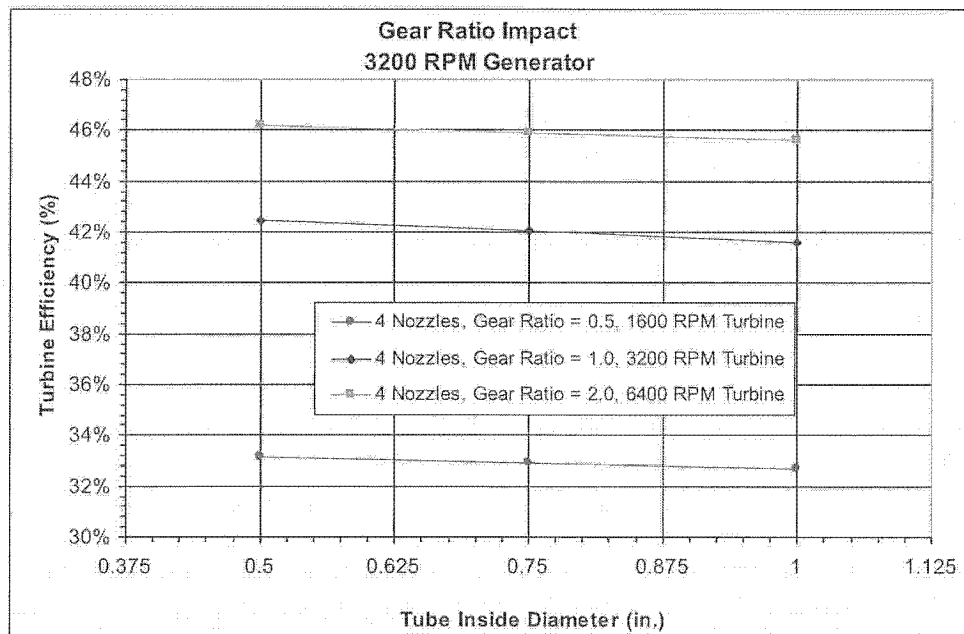3. cost limits for component and assembly manufacture (this may limit material sections).

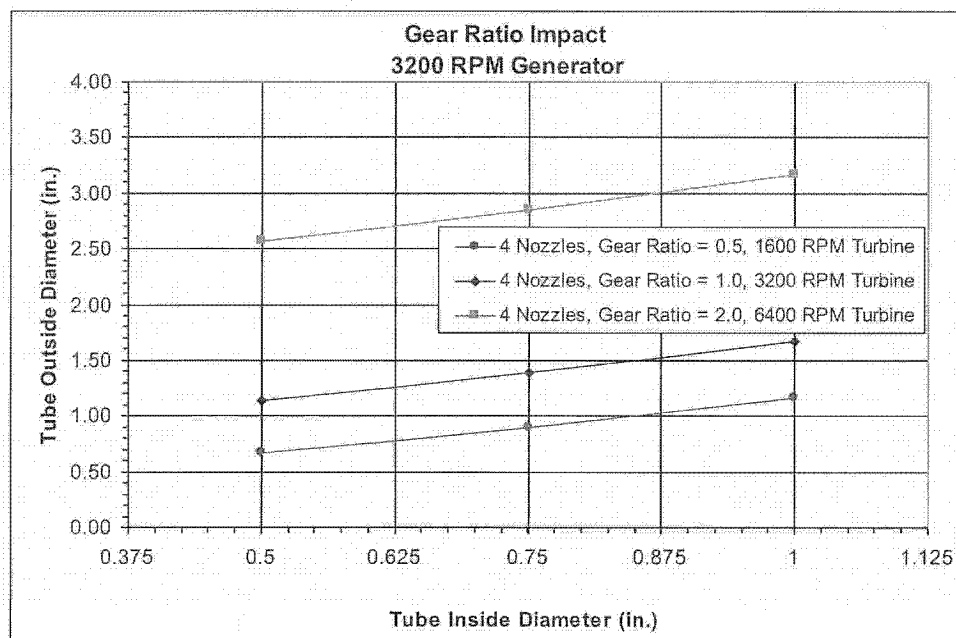**Figure 6. Effect of Gear Box Ratio on Turbine Efficiency**

Figure 7. Effect of Gear Box Ratio on Radial Tube Outside Diameter
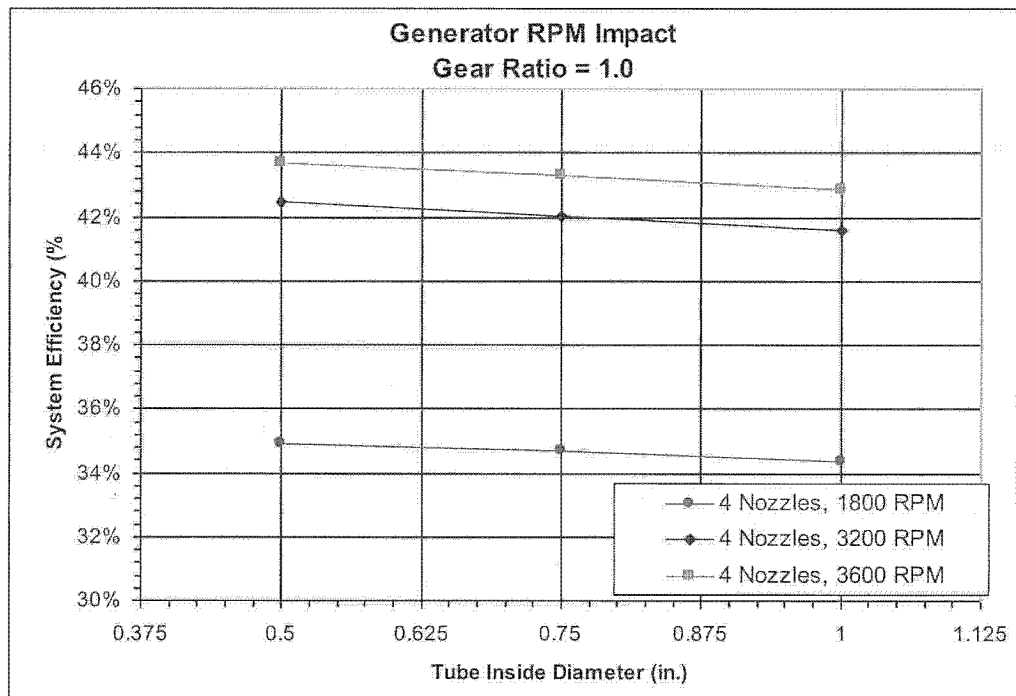
49

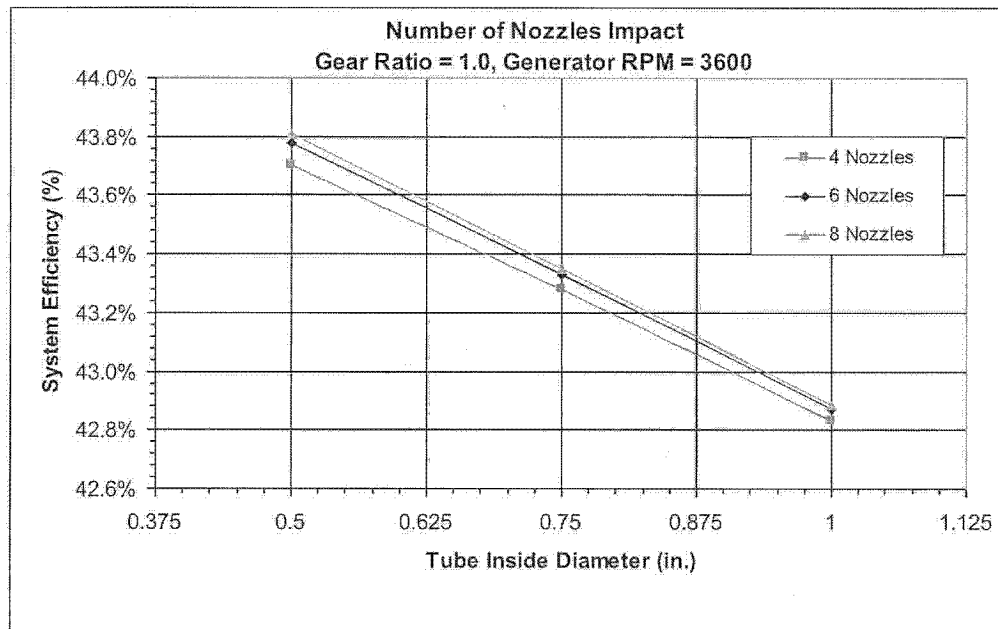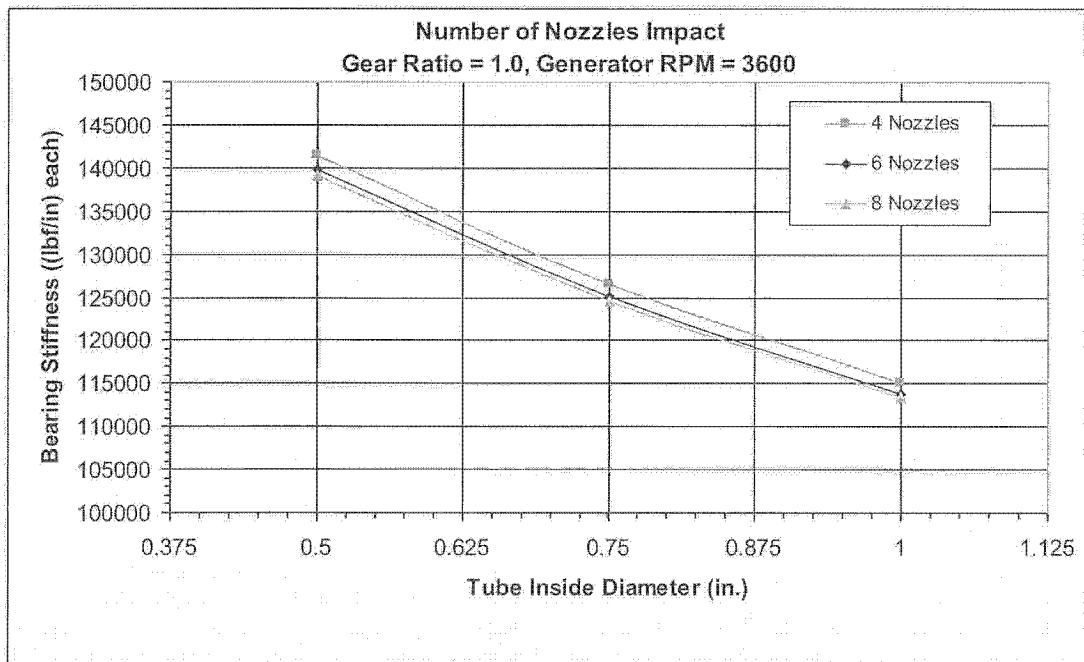Figure 8. Effect Of Generator Drive Speed on Turbine Efficiency

Figure 9. Effect of Exhaust Nozzle Quantity on Turbine Efficiency

50

Figure 10. Bearing Stiffness Requirement as Function of
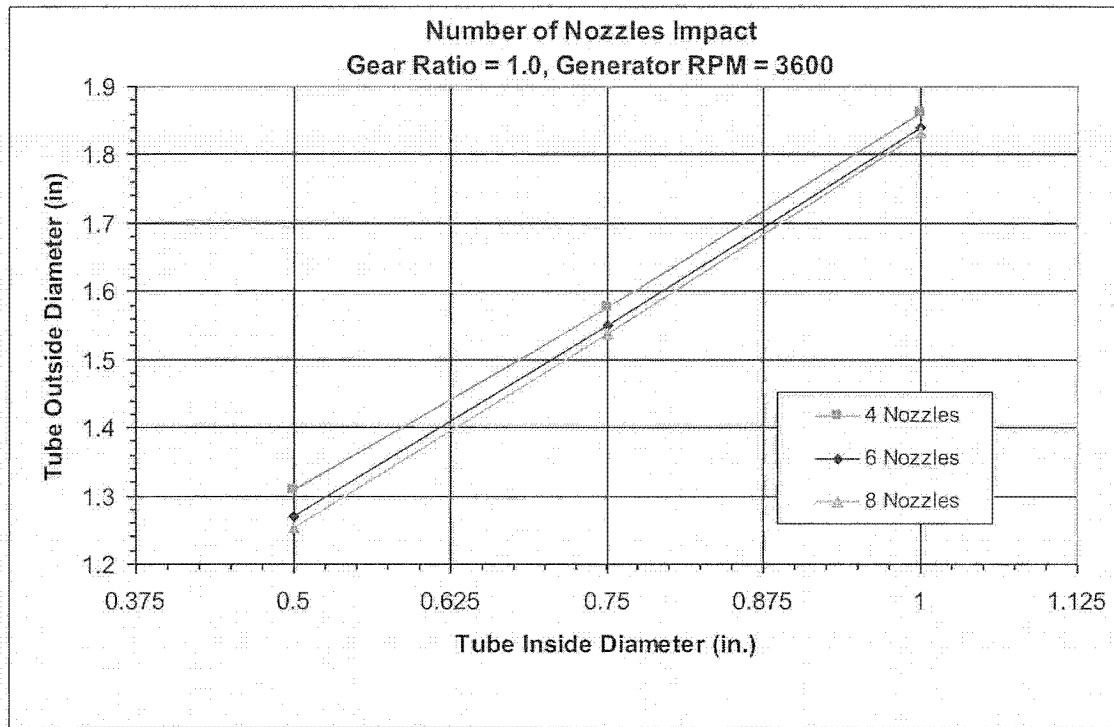Nozzle Quantity and Tube Internal Diameter

51

Figure 11. Effect of Exhaust Nozzle Quantity on Nozzle Feed Tube Outside Diameter

52

Table 2. Optimum Design Point for Conditions Considered

SYSTEM CHARACTERIZING PARAMETERS									
Power Output	No. of Steam Nozzles	Turbine Design Speed	Gear Box Ratio	Nozzle Radial Supply Tube Inner Diameter	Nozzle Radial Supply Tube Outer Diameter	Nozzle Centerline Radius	Disc Axial Width	Total Steam Flowrate	System Efficiency
(kW)		(RPM)		(in.)	(in.)	(in.)	(in.)	(lbm/sec)	(%)
1000	4	1800	1	0.5	0.702	44.6	0.772469	10.45	34.94%
1000	4	1800	1	0.75	0.937	44.6	1.030412	10.53	34.67%
1000	4	1800	1	1	1.202	44.0	1.322556	10.62	34.38%
1000	4	3200	1	0.5	1.132	29.1	1.245252	8.60	42.46%
1000	4	3200	1	0.75	1.396	29.0	1.535364	8.68	42.03%
1000	4	3200	1	1	1.677	28.8	1.844196	8.78	41.60%
1000	4	3600	1	0.5	1.309	26.1	1.440264	8.35	43.71%
1000	4	3600	1	0.75	1.577	26.0	1.734291	8.43	43.28%
1000	4	3600	1	1	1.860	25.9	2.046534	8.52	42.83%
1000	6	3600	1	0.5	1.271	26.2	1.397795	8.34	43.78%
1000	6	3600	1	0.75	1.550	26.0	1.704843	8.42	43.33%
1000	6	3600	1	1	1.840	25.9	2.024087	8.51	42.87%
1000	8	3600	1	0.5	1.254	26.2	1.379655	8.33	43.81%
1000	8	3600	1	0.75	1.538	26.1	1.692328	8.42	43.35%
1000	8	3600	1	1	1.832	25.9	2.014758	8.51	42.89%
1000	4	1600	0.5	0.5	0.674	48.1	0.741588	11.01	33.14%
1000	4	1600	0.5	0.75	0.900	47.9	0.990102	11.09	32.92%
1000	4	1600	0.5	1	1.168	47.5	1.284299	11.18	32.66%
1000	4	3200	1	0.5	1.132	29.1	1.245293	8.60	42.46%
1000	4	3200	1	0.75	1.396	29.0	1.535361	8.68	42.03%
1000	4	3200	1	1	1.677	28.8	1.844196	8.78	41.60%
1000	4	6400	2	0.5	2.567	14.4	2.823664	7.90	46.21%
1000	4	6400	2	0.75	2.853	14.3	3.138627	7.95	45.93%
1000	4	6400	2	1	3.173	14.3	3.490614	8.00	45.61%

53

Table 3. Predicted System Hydraulic Conditions for Configurations Listed in Table 2

| SYSTEM CHARACTERIZATION PARAMETERS | | | | | STEAM PRESSURE DROP | | | | | | | |
| Power Output | No. of Steam Nozzles | Turbine Design Speed | Gear Box Ratio | Nozzle Radial Supply Tube Inner Diameter | TOTAL PRESSURE DROP | Supply Port to Manifold | Manifold to Shaft Port | Shaft Port to Inner Shaft | Frictional Pressure Drop in Shaft | Shaft to Nozzle Feed Line Turn | Frictional Pressure Drop in Nozzle Feed Line | Nozzle Feed Line to Nozzle Turn |
(kW)		(RPM)		(in.)	(psid)	(psid)	(psid)	(psid)	(psid)	(psid)	(psid)	(psid)
1000	4	1800	1	0.5	139.860	0.146	3.831	0.975	0.032	31.623	86.912	16.342
1000	4	1800	1	0.75	34.775	0.144	0.000	0.350	0.032	6.276	11.206	16.766
1000	4	1800	1	1	38.258	0.133	0.010	0.246	0.033	1.946	2.637	33.255
1000	4	3200	1	0.5	79.294	0.000	2.042	0.692	0.101	21.179	38.714	16.566
1000	4	3200	1	0.75	33.012	0.000	0.000	0.200	0.104	3.830	5.012	23.866
1000	4	3200	1	1	37.345	0.000	0.007	0.123	0.107	0.894	1.198	35.015
1000	4	3600	1	0.5	71.807	0.014	1.779	0.583	0.142	19.909	32.793	16.586
1000	4	3600	1	0.75	32.880	0.017	0.001	0.149	0.146	3.277	4.253	25.037
1000	4	3600	1	1	37.233	0.022	0.010	0.086	0.150	0.701	1.018	35.247
1000	6	3600	1	0.5	40.287	0.013	0.022	0.249	0.142	8.416	14.822	16.624
1000	6	3600	1	0.75	36.997	0.017	0.004	0.104	0.145	1.120	1.947	33.660
1000	6	3600	1	1	39.601	0.021	0.028	0.217	0.150	0.120	0.471	38.593
1000	8	3600	1	0.5	33.212	0.013	0.000	0.172	0.141	4.312	8.475	20.099
1000	8	3600	1	0.75	38.283	0.016	0.012	0.103	0.145	0.486	1.125	36.396
1000	8	3600	1	1	41.012	0.021	0.044	0.282	0.149	0.065	0.274	40.177
1000	4	1600	0.5	0.5	161.361	0.190	4.422	1.016	0.026	35.394	104.071	16.242
1000	4	1600	0.5	0.75	37.633	0.185	0.001	0.368	0.026	6.962	13.307	16.784
1000	4	1600	0.5	1	38.468	0.178	0.011	0.261	0.027	2.204	3.147	32.641
1000	4	3200	1	0.5	79.294	0.000	2.042	0.692	0.101	21.179	38.714	16.566
1000	4	3200	1	0.75	33.012	0.000	0.000	0.200	0.104	3.830	5.012	23.866
1000	4	3200	1	1	37.345	0.000	0.007	0.123	0.107	0.894	1.198	35.015
1000	4	6400	2	0.5	47.825	1.459	0.501	0.025	1.691	11.143	16.164	16.842
1000	4	6400	2	0.75	35.596	1.494	0.015	2.613	1.719	0.023	2.091	27.641
1000	4	6400	2	1	43.163	1.538	0.074	3.378	1.757	0.171	0.500	35.745

IAUS Annual Solar-to-Electric Efficiency

As before mentioned, the long-term real data from CSP plants in the field is extensive. In the following section we will insert overlapping data from other CSP studies that apply to IAUS's CSP technology and combine these numbers with the efficiencies of both IAUS's Propulsion Turbine and Solar Panels to accurately view the net annual solar-to-electric efficiency of an IAUS solar power plant.

Annual Efficiency Data	SEGS VI	Solar Tres	Dish 10	IAUS
Solar Field Optical Efficiency	53.30%	56.00%	85.00%	83.79%
Receiver thermal efficiency	72.90%	78.30%	90.00%	90.00%
Transient effects	100.00%	100.00%	92.00%	92.00%
Piping loss efficiency	96.10%	99.50%	96.10%	96.10%
Storage Efficiency	100.00%	98.30%	100.00%	100.00%
Turbine power cycle efficiency	35.00%	40.50%	35.00%	43.50%
Electric loss efficiency	82.70%	86.40%	86.00%	86.00%
Power plant availability	98.00%	92.00%	94.00%	96.00%
Annual Solar to Electric Eff	10.59%	13.81%	19.14%	23.94%

(Table 1)

Table 1 gives a detailed efficiency comparison of IAUS's technology to other CSP technologies such as solar troughs (SEGS VI), solar dishes (Dish 10) and power towers (Solar Tres). It is a complete list of all the real energy losses CSP technologies encounter in the field. As Table 1 illustrates, there are many efficiency similarities between IAUS's CSP technology and the dish.

Solar Field Optical Efficiency
IAUS's solar field optical efficiency is more compatible to the dish due primarily to its dual-axis tracking capabilities. Table 2 breaks down the optical efficiency comparison between IAUS's system and the dish. The dish's mirror reflectivity of 93.5% is higher than IAUS's panel refraction transmittance of 90%, but unlike the dish, IAUS has no receiver interception. Although, due to the height and non-parabolic shape of IAUS's panel the affects of dust in the field appear to be less insidious than that of the dish, it is prudent to be conservative since IAUS's field data is not as thorough in relation to this factor. Therefore, we listed the affects of dust equal. In the end, the overall optical efficiencies of the two are very similar, the dish being nearly 1.8% higher.

Dish Optical Efficiency

Mirror Reflectivity	93.50%
Average Mirror Cleanliness	93.10%
Receiver Interception	98.00%
Overall Optical Efficiency	85.31%

IAUS Optical Efficiency

Panel Refraction Transmittence	90.00%
Average Cleanliness	93.10%
Receiver Interception	100.00%
Overall Optical Efficiency	83.79%

(Table 2)

Receiver Thermal Efficiency

The receiver thermal efficiency listed in Table 1 is virtually identical to the dish as well. Both have similar design features. They are both encapsulated, coated coils with greater surface area than other CSP technology receivers. IAUS hired out an independent review of its receiver, and not surprisingly, the results were the same as studies done for the dish.

SOLAR ENERGY RECOVERY OF ZINC OXIDE TO ZINC FOR ZINC AIR BATTERIES

The solar lens receiver system with the addition of an intermediate solar concentrator system the temperature at the receiver can exceed 2500° F. Using this system it is possible to break the oxygen bond from the zinc oxide to form zinc and oxygen. This process is extremely efficient use of the thermal energy produced from the solar lens system. The theoretic possibility is sixty percent efficient solar energy to zinc conversion. Zinc is an excellent fuel that can be used to produce electrical energy through the use of zinc fuel cell. The fuel cell converts the zinc back to zinc oxide and releases electrical energy in the process. To charge the zinc fuel cell just add zinc much like adding gasoline to the gas tank of an internal combustion engine. This system now makes it possible to produce transportation energy using solar energy where the storage is zinc. With the use of IAUS's unique lens technology and the compound parabolic mirror concentrator and the unique zinc oxide receiver system zinc can be produced economically while the specific heat of the process can still be used by IAUS's turbine to produce electricity.

Transient Clouds

The affects of transient clouds on the solar troughs and towers were included within the turbine power cycle efficiency numbers; therefore, in Table 1 these two are listed as zero loss. The dish studies had this portion broken out into its own category. Since IAUS's turbine cycle study did not include affects of transient clouds, it is listed out as well.

Piping Loss Efficiency

The piping loss efficiency of IAUS's system is similar to both the solar troughs and dish. The storage efficiency is

non-applicable to this study; therefore, it is listed as a 0% loss. IAUS will utilize heat storage in the future, however, it is not necessary to address it in this report.

Electric Loss Efficiency
The electric loss efficiency or parasitic load has more compatibility to the solar tower and the dish due to the piping configuration and other features.

Plant Availability
IAUS's plant availability lies between the solar dish and trough. It is higher than the dish due to IAUS's ability to economically install a redundant turbine back-up to switch on during routine turbine maintenance of the primary turbine. It is lower than the trough, however, due to the fact that the trough's numbers include a natural gas hybrid back-up. IAUS can use a natural gas hybrid configuration as well, but like the heat storage, it is not necessary to include it in this report.

Turbine Cycle Efficiency
IAUS's turbine power cycle efficiency is taken from its own independent review. The efficiency more closely resembles the solar tower due to higher temperature steam. However, as mentioned above the tower includes the losses from transient clouds in its turbine power cycle efficiency numbers, therefore, it is lower.

Conclusion

As addressed earlier in this report, IAUS is familiar with the material and construction cost of its system in the field. Based upon its low-cost design, IAUS's solar power plant needs to convert to electricity only 5% of the gross annual solar energy hitting its panels in order to compete with the lowest price solar technology available today. As detailed in this report, IAUS's annual solar-to-electric efficiency is nearly 24%. However, for argument's sake, even if we are to reduce IAUS's efficiency by 20%, which lowers it to an overall 20% annual solar-to-electric efficiency, it is still 400% higher than necessary to compete with the currently lowest price solar available.

Summary

IAUS believes that it has unprecedented advantages in nearly every area necessary for a renewable energy product to compete with fossil fuels such as a vast renewable resource, low cost equipment, durability, high-volume mass production capabilities, ease of construction, inexpensive and reliable energy storage, low cost operations, and longevity.

According to the International Energy Agency, over $11 Trillion will need to be invested into the global electricity market in order to bring electricity to the 1.6 billion people who currently live without power.

Currently, less than 1% of the world's energy comes from solar, yet the sun's energy is more abundant than all other energy sources combined and it's free. However, solar energy needs to reach a price of $1,500-$2,500 per KW in order to better compete with fossil fuels. IAUS'S solar power technology is expected to enter the market within this price range, but with room still to cut its costs again.

References

Zawadski and J Coventy. "Clean Energy? – Can Do!". Proceedings of Solar 2006. ANZSES annual conference, Canberra, Australia. 13-15 September 2006.

Sargent and Lundy 2003. "Assessment of Parabolic Trough and Power Tower Solar Technology Cost and Performance Forecasts" National Renewable Energy Laboratory, report NREL/SR-550-34440

GEF 2005. "Assessment of the World Bank / GEF strategy for the market development of solar thermal power" Global Environment Facility, World Bank, 2005

Cohen J et al 2006. Presentation on behalf of Solargenix, Proceedings of Solar 2006, ANZSES annual conference, Canberra, Australia, 13 - 15 September 2006.

Le Lievre P. 2006."Design of 6.5 MW solar thermal electricity plant with zero fossil fuel backup" Proceedings of Solar 2006, ANZSES annual conference, Canberra, Australia, 13 -15 September 2006

Lovegrove K. A. Luzzi, I. Soldiani and H. Kreetz "Developing Ammonia Based Thermochemical Energy Storage for Dish Power Plants." Solar Energy, 76 pp 331 – 337, 2003

Munzinger M. and Lovegrove K. "Biomass Gasification using Solar Thermal Energy". Proceedings of Solar 2006, ANZSES annual conference, Canberra, Australia, 13 -15 September 2006

Burgess G and Lovegrove K. "Solar thermal powered desalination: membrane versus distillation technologies". Proceedings of Solar 2005, ANZSES annual conference, Dunedin, New Zealand, November 2005